rich, SAP (SAF-A/B, Acinus, PIAS), and coiled-coil domains (7, 8). OTT-MAL encodes a fusion protein containing complete domain structures of both OTT and MAL. However, the molecular mechanism whereby this fusion protein induces leukemia is largely unknown. On the other hand, we and others have independently identified a murine homolog of MAL, referred to as BSAC and MRTF-A by functional cloning to inhibit tumor necrosis factor α-induced cell death and bioinformatics to identify related genes to myocardin, respectively (9, 10). Accumulating studies have shown that BSAC/MAL/MKL1/MRTF-A activates the promoters containing CArG boxes ($CC(A/T)_6GG$) through associating with serum response factor (SRF) (9–11). In addition, nuclear translocation of BSAC is tightly regulated by the Rho-actin signaling pathway (12). Although *BSAC/MAL/MKL1/MRTF-A* and *SRF* are broadly expressed in various tissues, the defect of *MKL1/MRTF-A*$^{-/-}$ mice is unexpectedly restricted to the development of the mammary gland (13, 14).

Yin Yang 1 (YY1) is a ubiquitous zinc finger transcription factor that binds to many different cellular and viral promoters in a sequence-specific manner to regulate transcription (15, 16). The mechanism by which YY1 activates or represses transcription largely depends on the interaction with other transcription factors or histone modification enzymes including TBP, TAFs, SP1, p300, and HDACs (15, 16). Importantly, the targeted disruption of *YY1* resulted in preimplantation lethality, indicating that YY1 is essential for mouse embryo development (17). Moreover, subcellular localization of YY1 is regulated in a cell cycle-dependent fashion and modulates the function of the cell cycle control genes including *Rb* and *p53*. Furthermore, a recent study has revealed that perturbed expression of YY1 inhibits maturation of granulocytes, suggesting an intimate link with the development of acute myeloid leukemia (18). Collectively, YY1 potentially controls the expression of vast array of genes that are important in basic cellular processes such as DNA replication, transcription, and cell cycle control and also involved in the leukemogenesis.

Given that the promoters containing CArG boxes are found in immediate early genes or muscle-specific genes and OTT-BSAC is involved in the development of leukemia, we speculated that OTT-BSAC activates promoter(s) containing a motif other than CArG box. We found that OTT-BSAC strongly activated the promoters of human platelet collagen receptor glycoprotein VI (*GPVI*) gene. Deletion and mutation analysis revealed that OTT-BSAC-mediated transcriptional activity depended on the YY1-binding sequences. Interestingly, in contrast to BSAC, which predominantly localized in the cytoplasm and the nuclear translocation of which is tightly regulated by the Rho-dependent signals (12), OTT and OTT-BSAC exclusively localized in the nucleus. The constitutive nuclear accumulation of OTT-BSAC may contribute to a significant enhancement of its transcriptional activity. Moreover, OTT interacted with HDAC3, and this interaction was abolished in OTT-BSAC. Collectively, these functional and spatial alterations of OTT and BSAC may culminate in the development of leukemia.

EXPERIMENTAL PROCEDURES

Reagents and Cell Culture—Anti-FLAG (Sigma-Aldrich), anti-hemagglutinin (Roche Applied Science), anti-Myc, anti-GAL4, and anti-YY1 (Santa Cruz Biotechnology), anti-HDAC3 (Biomol), anti-β-actin (BioLegend) antibodies, control mouse IgG (BD Biosciences), and control rabbit IgG (Sigma-Aldrich) were purchased from the indicated sources. HEK293 and HEK293T cells were cultured in high glucose Dulbecco's modified Eagle's medium containing 10% fetal calf serum. Megakaryocytic leukemic cell lines, CMS and CMY (T. Sato), and MEG-01 cells (M. Seto) (19) were kindly provided and cultured in RPMI1640 medium containing 10% fetal calf serum. Anti-OTT antibody was generated by immunizing rabbits with GST-OTT (609–730). Anti-BSAC antibody was generated and described previously (9).

Plasmids—pBJ5-FLAG-HDAC1 (S. Schreiber), pME18S-FLAG-HDAC2 and pCEP4-FLAG-HDAC3 (E. Seto), and pCMX-mSMRTα-FL (R. M. Evans) were kindly provided from the indicated researchers. pCR-FLAG-YY1 was constructed by PCR using pCR-YY1 as a template (20). pCR-FLAG-HDAC3ΔN and pCR-FLAG-HDAC3ΔC were constructed by deleting N-terminal 307 and C-terminal 121 amino acids using PCR, respectively. A full-length *OTT* cDNA was isolated by screening a library derived from human HTLV-1-transformed T cell line HAT109 as a standard procedure. To express full-length and various deletion mutants of OTT as fusion proteins with DNA-binding domain of a yeast transcriptional factor GAL4, PCR products encoding the indicated amino acids were subcloned into pFA vector (Stratagene), designated as pFA-OTT, pFA-OTT(1–677), pFA-OTT(654–957), pFA-OTT(609–730), and pFA-OTT(1–533). pcDNA3-Myc-OTT was constructed by PCR and subcloned into pcDNA3-Myc vector. pcDNA3-Myc-human BSAC and pCR-FLAG-human HDAC6 were constructed by PCR using KIAA1438 (human *BSAC/MAL/MKL1/MRTF-A*) and KIAA0901 (human *HDAC6*) cDNAs derived from the Kazusa DNA Institute as templates, respectively. To make an expression vector for OTT-BSAC, PCR products of *OTT* and *BSAC* were connected by creating an additional EcoRI site at the fusion junction and ligated to pcDNA3-Myc vector. The artificially created EcoRI site was subsequently mutated to the originally published sequence of the *OTT-BSAC* fusion junction using a QuikChange site-directed mutagenesis kit (Stratagene). Expression vectors for C-terminal deletion mutants of OTT-BSAC (−351) and OTT-BSAC (−537) were constructed by using the internal restriction enzyme sites XmnI and BsgI to delete C-terminal fragments, respectively. The numbers indicate deleted amino acids from the C terminus of OTT-BSAC.

Reporter Assay—The promoter of the human *GPVI* gene (−315 to +29) was amplified by PCR using human genomic DNA as a template and subcloned into pGL3-basic vector (Promega), designated as pGL3-*GPVI* (−315/+29). A series of 5′ deletion mutants, pGL3-*GPVI* (−207/+29), pGL3-*GPVI* (−79/+29), and pGL3-*GPVI* (−39/+29) were generated by PCR using pGL3-*GPVI* (−315/+29) as a template. pGL3-*GPVI* (−208/+29M1), pGL3-*GPVI* (−208/+29M2), and pGL3-*GPVI* (−79/+29M3) were generated by introducing mutations

of GATA (AGATAA to CGCTTA), the first YY1 (GATGAG to GCTTAG), and third YY1 (CTCATC to CTAAGC) binding sites, respectively. Reporter plasmids, pGL3-c-*fos* (−700/+53), pGL3-*FcεRIα* (−605/+29), and mPGV-B-*il-6* (−181/+14) were described previously (9, 20, 21). Luciferase assays using HEK293 and HEK293T cells were performed as previously described (22). MEG-01 cells (2×10^5) were transfected with the indicated expression vectors along with reporter plasmids using Lipofectamine 2000 (Invitrogen). After 48 h, the cells were harvested, and the luciferase activities were measured on a luminometer (Berthold).

Electrophoretic Mobility Shift Assay (EMSA)—EMSA was performed as previously described (20). Briefly, 5 μg of the nuclear extracts were incubated with the rhodamine-labeled wild-type oligonucleotides in the absence or presence of anti-YY1 antibody, wild-type, or mutant cold competitors with a 10–100-fold excess. The oligonucleotides used were as follows: wild-type sense oligonucleotide for *GPVI*, 5′-AGGAAGGGAGGAGAGCATTCTTCATCCTCATCACATCCTG-3′; mutant sense oligonucleotide, 5′-AGGAAGGGAGGAGAGCATTCTTCATCCTAAGCGCATCCTG-3′. Mobility shift of the complexes was analyzed by a fluorescence detector, FMBIO-100 (Takara Shuzo).

Chromatin Immunoprecipitation (ChIP) Assay—The ChIP assay was performed using a ChIP Assay kit (Millipore) as previously described (23). Quantitative PCRs were performed using TaqMan Universal PCR master mix and a 7500 Real-Time PCR system (Applied Biosystems). The primers to amplify the promoter region of *GPVI* gene (−127/+29) and a TaqMan probe were as follows: Forward primer (5′-GGCTACGGCTCGATGAGTCTC-3′), reverse primer (5′-TCAGCCCTGTCCTGAGCTCT-3′), and a TaqMan probe (5′-FAM-TTCATCCTCATCACATCC-MGB-3′). The amount of target DNA bound to YY1 or OTT-BSAC was quantified using immunoprecipitates with control, anti-YY1, or anti-Myc antibodies from the cycle threshold value, which was determined using 7500 SDS software (Applied Biosystems). In brief, the ratio of the amount of a specific DNA fragment in each immunoprecipitate to the amount of that fragment in the DNA before immunoprecipitation (input DNA) was calculated from each cycle threshold value.

Subcellular Fractionation, Immunoprecipitation, and Immunoblotting—HEK293 cells (4×10^6) were transiently transfected with the indicated expression vectors using Lipofectamine (Invitrogen). MEG-01 cells (4×10^6) were untreated or transfected with the indicated expression vectors using a nucleofector according to the manufacturer's instructions (Amaxa). For subcellular fractionation, the cells were harvested at 24–36 h after transfection and washed with 1 ml of a buffer A (10 mM Hepes, pH 7.9, 1.5 mM $MgCl_2$, 10 mM KCl, 1 μg/ml aprotinin, 1 μg/ml leupeptin, 1 mM dithiothreitol, and 1 mM phenylmethylsulfonyl fluoride) and then resuspended in 500 μl of the buffer A. After incubation for 30 min, the cells were passed with a 30-gauge syringe 10 times, followed by centrifugation at 700 × *g*. The supernatants were further centrifuged at 15,000 × *g* to remove insoluble pellets, and the resulting supernatants were collected as the cytoplasmic fractions. The pellets were resuspended in 100 μl of buffer B (20 mM Hepes, pH 7.9, 450 mM NaCl, 1.5 mM $MgCl_2$, 25% glycerol, 0.2 mM EDTA, 1 μg/ml aprotinin, 1 μg/ml leupeptin, 1 mM dithiothreitol, and 1 mM phenylmethylsulfonyl fluoride) for 60 min. After centrifugation at 15,000 × *g* for 10 min, the supernatants were collected as the nuclear fractions. Equal amounts of proteins from each fraction were subjected to SDS-PAGE and transferred onto polyvinylidine difluoride membranes (Millipore). The membranes were incubated with the indicated antibodies followed by the corresponding secondary antibodies. The membranes were then developed with the ECL Western Blotting Detection System Plus (GE Healthcare).

Small Interfering RNAs (siRNAs)—HEK293T cells (2.5×10^5) were transfected with siRNAs targeting green fluorescent protein (control) or *YY1* (ON-TARGETplus SMARTpool siRNA, Dharmacon) and pGL3-*GPVI* (−315/+29) along with Myc-OTT-BSAC using Lipofectamine 2000 (Invitrogen). After 48 h, knockdown of YY1 was evaluated by immunoblotting with anti-YY1 antibody using total lysates, and luciferase assay was performed as previously described (22).

Immunostaining—MEG-01 cells (4×10^6) were untreated or transfected with the indicated expression vectors and plated on glass slides. After 24 h, the cells were washed with phosphate-buffered saline, fixed with 2% paraformaldehyde, and then incubated with anti-OTT, anti-BSAC, and anti-Myc antibodies. The primary antibodies were detected by secondary antibodies conjugated with Alexa 488 or Alexa 594 (Invitrogen). To visualize the nuclei, the cells were incubated with Hoechst 33258 (Invitrogen). Stained cells were mounted in SlowFade (Invitrogen) and analyzed on a laser scanning confocal microscope (Zeiss).

RESULTS

Identification of a Novel Target Gene Activated by the Fusion Protein OTT-BSAC—OTT-MAL encodes a fusion protein containing complete domain structures of both OTT and MAL (Fig. 1*A*). However, the molecular mechanism whereby this fusion protein induces leukemia is largely unknown. Given that CArG boxes are found in the promoters of immediate early genes or muscle-specific genes, we speculated that OTT-BSAC should control gene(s) that might be responsible for the development of leukemia. Given that OTT-BSAC might impair the differentiation of megakaryocytes, we first tested whether OTT-BSAC could affect the promoter activity of megakaryocyte-specific genes. A previous study has shown that *GPVI* is specifically expressed in megakaryocytes and platelets (24). Then we generated a reporter plasmid containing the *GPVI* promoter upstream of a luciferase gene. We transfected megakaryocytic leukemic cell line MEG-01 cells with expression vectors for BSAC, OTT, and OTT-BSAC along with a reporter plasmid, pGL3-*GPVI* (−315/+29), and tested the effect of each protein on this promoter activity. Expression of BSAC or OTT did not significantly increase this promoter activity (Fig. 1*B*), which is consistent with the fact that this promoter does not contain a CArG box. Surprisingly, expression of OTT-BSAC strongly activated this promoter in a dose-dependent fashion (Fig. 1*B*). This OTT-BSAC-mediated transcriptional activation of the *GPVI* promoter was also observed in HEK293 cells (Fig. 1*B*). To investigate whether OTT-BSAC-dependent transcriptional activity on the *GPVI* promoter is

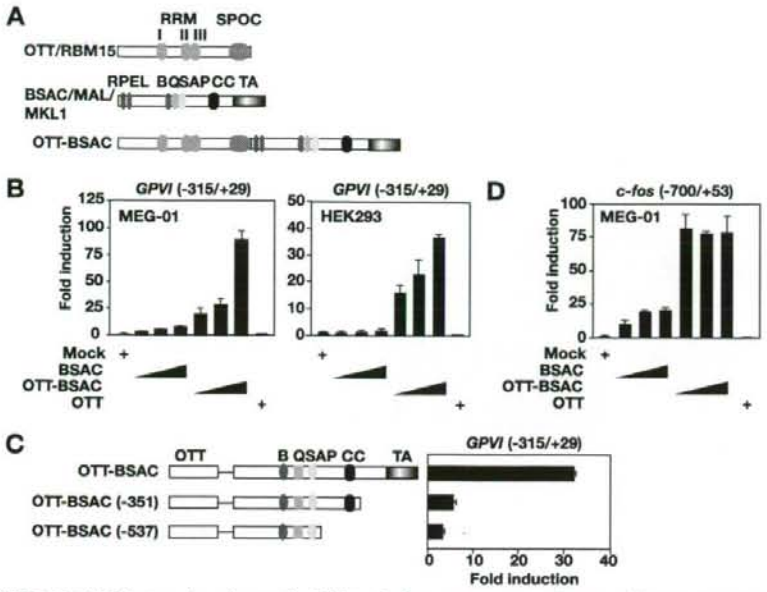

FIGURE 1. **OTT-BSAC strongly activates the *GPVI* and c-*fos* promoters.** *A*, a diagram of domain structures of OTT/RBM15, BSAC/MAL/MKL1/MRTF-A, and OTT-BSAC. RNA recognition motif, SPOC, RPEL, basic (*B*), glutamine-rich (*Q*), SAP, coiled-coil (*CC*), and TA domains are shown. *B*, MEG-01 and HEK293 cells were transfected with increasing amounts of the indicated expression vectors along with pGL3-*GPVI* (−315/+29). Luciferase activities are expressed as fold increases above that with control vector. Each experiment was performed in triplicate, and the results are expressed as the means ± SE of three experiments. *C*, MEG-01 cells were transfected activities are expressed as in *B*. *D*, MEG-01 cells were transfected with increasing amounts of the indicated expression vectors along with pGL3-c-*fos* (−700/+53). Luciferase activities are expressed as in *B*.

mediated by the transcriptional activation (TA) domain of BSAC, we transfected MEG-01 cells with deletion mutants of OTT-BSAC lacking the TA domain. Although the expression levels of two OTT-BSAC mutants lacking the TA domain were comparable with OTT-BSAC (supplemental Fig. S1), two mutants failed to activate this promoter (Fig. 1*C*). This indicates that the TA domain of BSAC mediates transcriptional activity of OTT-BSAC. Given that protein expression levels of OTT-BSAC were consistently lower than BSAC, possibly because of its large molecular mass of OTT-BSAC (supplemental Fig. S1), increased transcriptional activity of OTT-BSAC is not due to the increased protein expression levels. Consistent with a previous study (11), we also observed significant enhancement of transcriptional activity of OTT-BSAC on the c-*fos* promoter compared with BSAC (Fig. 1*D*). Given that the *GPVI* but not c-*fos* promoter does not contain CArG box, these results suggest that OTT may directly or indirectly recruit BSAC to the *GPVI* promoter, resulting in up-regulation of the *GPVI* promoter activity.

Transcriptional Activation by OTT-BSAC Depends on the YY1-binding Sequences—To identify a target sequence recognized by OTT-BSAC, we constructed a series of 5′ deletion mutants of the *GPVI* promoter (Fig. 2*A*). Although deletion up to the position −208 did not impair the transcriptional activity induced by OTT-BSAC, further deletion up to −80 reduced the transcriptional activity to ~50% (Fig. 2*B*). Moreover, deletion up to −40 resulted in complete loss of the transcriptional activation. These results indicate that the regions spanning −207 to −80 and −79 to −40 are essential for OTT-BSAC-mediated transactivation. A previous study has shown that the *GPVI* promoter activity is regulated by Sp1, GATA, and Ets motifs (24). In addition, we found three putative YY1-binding sequences (designated as YY1-I, YY1-II, and YY1-III) in the *GPVI* promoter (Fig. 2*A*). We tested whether the mutation of these sites impairs OTT-BSAC-mediated transactivation. The mutation of the GATA-binding sequence did not reduce but rather enhanced the transcriptional activity. Unexpectedly, mutation of YY1-I reduced the transcriptional activity comparable with a deletion mutant (−79/+29) (Fig. 2*B*). Furthermore, the mutation of YY1-III substantially reduced the transcriptional activity 5-fold. Notably, combined mutations of YY1-III along with Ets motifs or YY1-II did not further reduce the transcriptional activity compared with YY1-III mutation alone (data not shown). Combining these data together indicates that YY1-I and YY1-III sequences are essential for OTT-BSAC-dependent transcriptional activation.

We next tested whether YY1 actually binds to the promoter by EMSA. We prepared the nuclear extracts from MEG-01 cells and performed EMSA using double-stranded oligonucleotides (oligonucleotides) containing a region spanning −79 to −40 as a probe. As shown in Fig. 2*C*, two major retarded bands (designated the complex I and II hereafter) were detected in this assay, and these two bands disappeared by the addition of the nonlabeled wild-type oligonucleotides. In contrast, the addition of the mutant probe, in which YY1-binding core sequence (TCAT) was mutated to TAAG, did not abolish the binding of the two complexes to the labeled oligonucleotides, indicating that these complexes specifically bound to TCAT sequence. Moreover, complex II but not complex I disappeared in the presence of anti-YY1 antibody, suggesting that complex II contains YY1. Collectively, YY1 binds to the *GPVI* promoter via TCAT sequence. However, we could not detect direct interaction of YY1 with BSAC or OTT in cotransfection experiments or a ternary complex containing YY1 and BSAC or OTT-BSAC in the presence of YY1-binding sequence in EMSAs (data not shown).

To directly show that endogenous YY1 is recruited to the *GPVI* promoter under more physiological conditions, we performed ChIP assays. Consistent with EMSAs, anti-YY1 but not control antibody efficiently immunoprecipitated the *GPVI* promoter from HEK293T and MEG-01 cells (Fig. 2*D*). However, the relative intensities of the *GPVI* promoter using immunoprecipitates with anti-Myc antibody were not different in between mock and Myc-OTT-BSAC-transfected HEK293T cells (Fig. 2*E*). This suggests that the recruitment of transfected

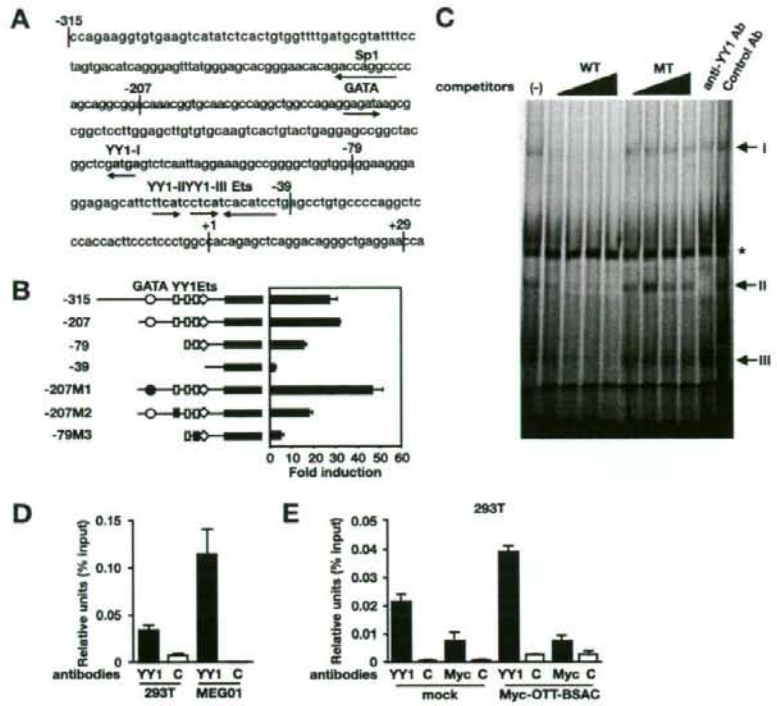

FIGURE 2. **OTT-BSAC activates the *GPVI* promoter via the YY1-binding motifs.** *A*, the promoter region of human *GPVI* gene. The putative transcriptional factor binding sites are *underlined* by the *arrows* showing its orientation (sense or antisense orientation). +*1* indicates the transcription start site. The putative YY1-binding sequences are indicated by *bold characters*. *B*, delineation of the regions required for OTT-BSAC-dependent transactivation. MEG-01 cells were transfected with OTT-BSAC along with the indicated mutants of pGL3-*GPVI* reporter vector. Luciferase activities are expressed as in Fig. 1*B*. *M1*, *M2*, and *M3* are the mutants, in which GATA1, the first YY1, and third YY1 motifs were mutated, respectively. *C*, YY1 specifically binds to the promoter of *GPVI*. The nuclear extracts were incubated with the rhodamine-labeled wild-type oligonucleotides containing the *GPVI* promoter (−79 to −39) in the absence or presence of increasing amounts of the nonlabeled wild-type (*WT*) or mutant (*MT*) oligonucleotides or anti-YY1 or control antibodies. The retarded bands are indicated by *arrows*. The *asterisk* indicates nonspecific bands. *D*, *in vivo* binding of YY1 to the *GPVI* promoter in HEK293T and MEG-01 cells. The binding of YY1 to the *GPVI* promoter region (−127/+22) was quantified using ChIP assays. The results are expressed as the means ± S.D. of three independent PCRs with duplicates samples. *E*, OTT-BSAC does not bind to the *GPVI* promoter *in vivo*. Mock or Myc-OTT-BSAC-transfected HEK293T cells were subjected to ChIP assays using anti-YY1, anti-Myc, or control antibodies. The results are expressed as in *D*.

OTT-BSAC to the *GPVI* promoter could not be detected, at least under our experimental conditions.

YY Is Not Essential for OTT-BSAC-dependent Transcriptional Activation—Previous studies have shown that myocardin and BSAC do not directly bind to the promoters containing CArG boxes but activates them through interaction with SRF (9–11). Under these conditions, transcriptional activities by myocardin and BSAC are extremely sensitive to the levels of SRF, because high concentration of SRF does not enhance but rather attenuates myocardin- or BSAC-dependent transcriptional activation (25).[3] To test whether similar interplay between OTT-BSAC and YY1 is also observed on the *GPVI* promoter, we examined whether expression of YY1 attenuates OTT-BSAC-dependent transactivation. Although expression of YY1 alone weakly activated this promoter, expression of YY1 substantially inhibited OTT-BSAC-mediated transcriptional activation in a dose-dependent fashion (Fig. 3*A*). Notably, this inhibitory effect of YY1 was promoter-specific, because expression of YY1 only weakly inhibited OTT-BSAC-dependent transactivation on the c-*fos* promoter (Fig. 3*B*). We confirmed that the expression levels of transfected YY1 in the *GPVI* promoter-transfected MEG-01 cells were nearly identical to those of c-*fos* promoter-transfected MEG-01 cells (Fig. 3*C*).

The fact that YY1 substantially suppressed OTT-BSAC-mediated transcriptional activation raises two possibilities. One is that YY1 may recruit OTT-BSAC to the *GPVI* promoter, although the recruitment of transfected OTT-BSAC to the *GPVI* promoter was not detected under our experimental conditions (Fig. 2*E*). The other is that a transcription factor other than YY1 recruits OTT-BSAC to the YY1-binding sequences and activates the *GPVI* promoter; therefore YY1 appears to suppress OTT-BSAC-dependent transcriptional activation through competitive binding inhibition (Fig. 3*A*). To discriminate these two possibilities, we knocked down endogenous YY1 using siRNA and tested whether OTT-BSAC-dependent transcriptional activation is abolished in YY1-knockdown HEK293T cells. Although *YY1* siRNA efficiently knocked down expression of YY1, OTT-BSAC-mediated transcriptional activation was not impaired (Fig. 3*D*). Collectively, OTT-BSAC activates transcription on the *GPVI* promoter through the YY1-binding sequences, but YY1 is not essential for OTT-BSAC- mediated transcriptional activation.

We finally investigated whether OTT-BSAC activates other promoters containing the YY1-binding sequences. We have previously shown that the human *FcεRIα* subunit promoter contains the YY1-binding sequences and is activated by YY1 (20). Thus, we tested whether expression of OTT-BSAC activates this promoter. As expected, OTT-BSAC substantially increased this promoter activity (Fig. 3*E*). We also found that OTT-BSAC activates the murine *il-6* promoter, which also contains the YY1-binding sequences (Fig. 3*E*).

The Signal-independent Nuclear Accumulation of OTT-BSAC—To elucidate the mechanism whereby transcriptional activity of OTT-BSAC is enhanced compared with BSAC, we speculated that OTT fusion to BSAC could affect the subcellular localization of BSAC. We first examined the subcellular

[3] T. Sawada and H. Nakano, unpublished results.

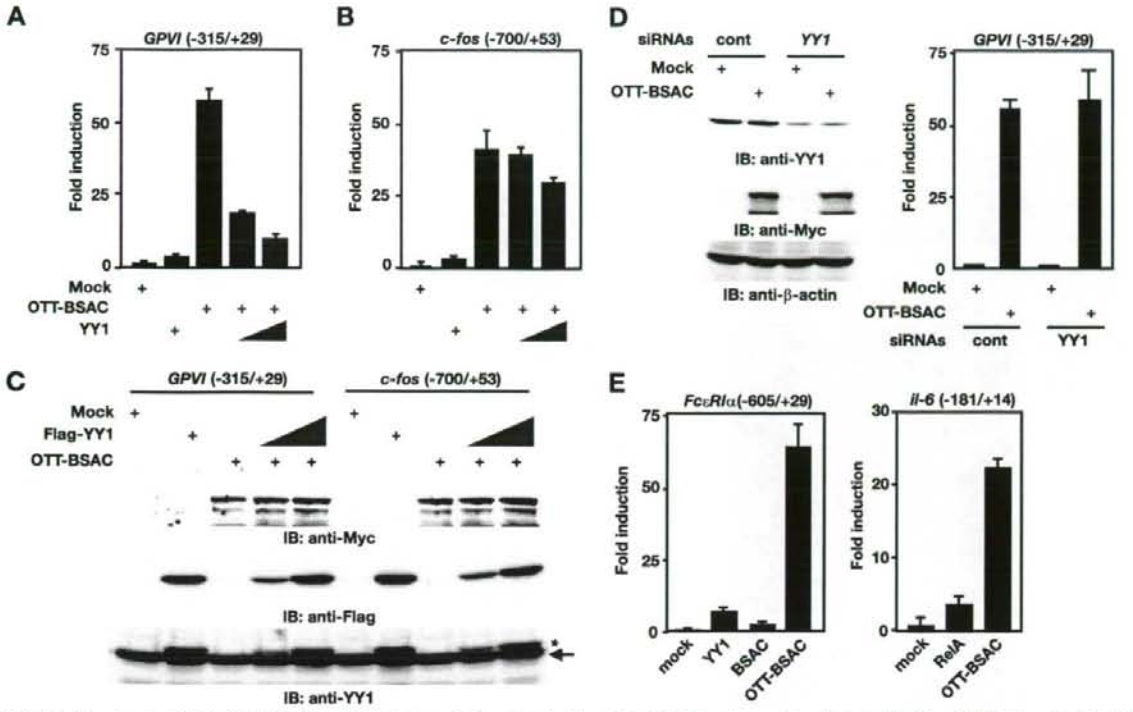

FIGURE 3. **YY is not essential for OTT-BSAC-mediated transcriptional activation.** *A–C*, MEG-01 cells were transfected with Myc-OTT-BSAC and pGL3-*GPVI* (−315/+29) (*A* and *C*) or pGL3-*c-fos* (−700/+53) (*B* and *C*) along with increasing amounts of FLAG-YY1. The luciferase activities are expressed as in Fig. 1*B*. *C*, expression levels of transfected proteins and endogenous YY1 were detected by immunoblotting (*IB*) with anti-Myc, anti-FLAG, and anti-YY1 antibodies. The *arrow* and *asterisk* indicate endogenous and transfected YY1, respectively. *D*, knockdown of YY1 using siRNA does not impair OTT-BSAC-dependent transcriptional activation. HEK293T cells were transfected with siRNAs targeting green fluorescent protein (control) or *YY1* and pGL3-*GPVI* (−315/+29) along with an empty vector (mock) or Myc-OTT-BSAC. After 48 h, the expression levels of endogenous YY1 and transfected OTT-BSAC were detected by immunoblotting with anti-YY1 (*top panel*) and anti-Myc antibodies (*middle panel*), respectively. The equal loading of the samples was verified by immunoblotting with anti-β-actin antibody (*bottom panel*). The luciferase activities are expressed as in Fig. 1*B*. *E*, MEG-01 cells were transfected with the indicated expression vectors along with pGL3-*FcεRIα* (−605/+29) or mPGV-B-*il-6* (−181/+14). The luciferase activities are expressed as in Fig. 1*B*.

localization of endogenous BSAC and OTT in MEG-01 cells. Consistent with a previous study (12), endogenous BSAC predominantly localized in the cytoplasm with a minor population in the nucleus (Fig. 4*A*). To investigate the subcellular localization of endogenous OTT, we generated anti-OTT antibody. This antibody recognized endogenous OTT with a molecular mass of 120 kDa in the whole cell lysates from MEG-01, HeLa, HEK293, and Jurkat T, but not CMS or CMY cells (Fig. 4*C*). Consistent with a very recent study, in which ectopically expressed OTT localizes in the nucleus (26), endogenous OTT localized in the nucleus (Fig. 4*A*). Similarly, transfected BSAC and OTT showed identical subcellular distribution patterns to endogenous BSAC and OTT, respectively (Fig. 4*B*). We finally investigated the localization of OTT-BSAC. Because leukemia cell line(s) from patients with acute megakaryoblastic leukemia are not currently available, we transiently transfected MEG-01 cells with Myc-OTT-BSAC. Interestingly, OTT-BSAC exclusively localized in the nucleus (Fig. 4*B*).

To evaluate the subcellular localization of OTT, BSAC, and OTT-BSAC more quantitatively, we separated the cells into the cytoplasmic and nuclear fractions and detected each protein in the fractions by using Western blotting. Consistent with the results using a confocal microscopy, endogenous and transfected OTT mainly localized in the nucleus (Fig. 4, *D* and *E*). Although endogenous and transfected BSAC predominantly localized in the cytoplasm and the small population of BSAC localized in the nucleus, transfected OTT-BSAC exclusively localized in the nucleus. Collectively, OTT fusion to BSAC drastically changed the subcellular localization of BSAC. This might be one of the molecular mechanisms underlying the aberrant up-regulation of OTT-BSAC-dependent transcriptional activity.

OTT Interacts with HDAC3—A previous study has shown that SHARP interacts with HDACs, SMRT, and N-CoR and acts as a transcriptional repressor (5). OTT has a structural similarity to SHARP (5, 6), prompting us to test whether OTT interacts with HDACs. We transiently transfected HEK293 cells with Myc-OTT along with FLAG-HDAC1, -2, or -3. The lysates were immunoprecipitated with anti-Myc antibody, and co-immunoprecipitated HDACs were detected by anti-FLAG antibody. HDAC3, but not HDAC1 or HDAC2, was specifically co-immunoprecipitated with OTT (Fig. 5*A*). In contrast, BSAC could not bind to HDAC3. A reciprocal immunoprecipitation experiment showed that OTT was also co-immunoprecipitated with HDAC3 (Fig. 5*A*). On the other hand, OTT did not interact with HDAC6, a member of the class II HDAC family (data

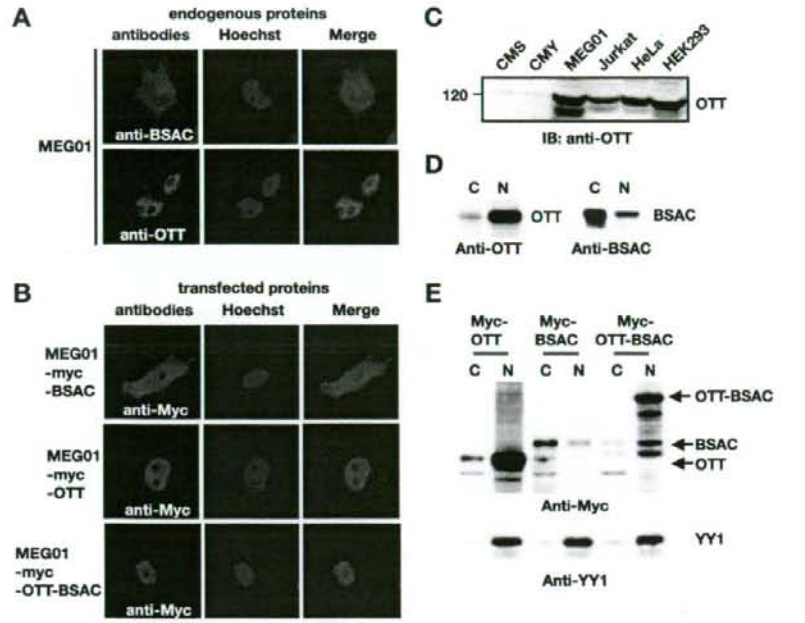

FIGURE 4. **Signal-independent nuclear accumulation of OTT-BSAC.** *A* and *B*, MEG-01 cells were untransfected (*A*) or transfected (*B*) with Myc-BSAC, Myc-OTT, or Myc-OTT-BSAC. Then the cells were stained with anti-BSAC (*A*), anti-OTT (*A*), or anti-Myc (*B*) antibodies and analyzed by a confocal microscopy. The nuclei were stained with Hoechst 33258 (*blue*) and the merged images are represented at the *right*. *C*, expression of OTT in various cell lines. Expression levels of endogenous OTT were analyzed by immunoblotting (*IB*) with anti-OTT antibody. The relative molecular mass (kDa) is indicated at the *left*. *D*, subcellular fractionation of endogenous OTT and BSAC in MEG-01 cells. Subcellular fractionation was performed as described under "Experimental Procedures," and equal amounts of proteins were subjected to SDS-PAGE. The expression levels of OTT and BSAC were analyzed by immunoblotting with anti-OTT and anti-BSAC antibodies, respectively. *C* and *N* indicate the cytosolic and nuclear fractions, respectively. *E*, subcellular localization of transfected Myc-OTT, Myc-BSAC, and Myc-OTT-BSAC. MEG-01 cells were transfected with the indicated vectors, and the subcellular fractionation and SDS-PAGE were performed as in *D*. Expression levels of transfected proteins in each fraction were analyzed by immunoblotting with anti-Myc antibody (*top panel*). The equal loading of the nuclear extracts was verified by immunoblotting with anti-YY1 antibody (*bottom panel*).

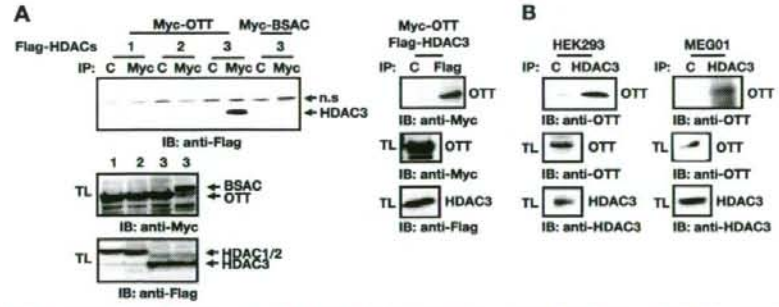

FIGURE 5. **OTT physically interacts with HDAC3.** *A*, OTT interacts with HDAC3, but not HDAC1 or HDAC2. HEK293 cells were transfected with the indicated expression vectors. After immunoprecipitation (*IP*) with control (*lane C*), anti-Myc, or anti-FLAG antibodies, co-immunoprecipitated proteins were detected by immunoblotting (*IB*) with anti-FLAG or anti-Myc antibodies (*top panel*). Expression levels of the transfected proteins in the total lysates (*TL*) were analyzed by immunoblotting with anti-Myc or anti-FLAG antibodies, respectively (*middle* and *bottom panels*). The *numbers 1*, *2*, and *3* indicate HDAC1, HDAC2, and HDAC3, respectively. *B*, endogenous interaction of OTT with HDAC3 in HEK293 and MEG-01 cells. After immunoprecipitation with control (*lane C*) or anti-HDAC3 antibodies, co-immunoprecipitated OTT was detected by immunoblotting with anti-OTT antibody (*top panels*). Expression levels of endogenous OTT and HDAC3 in the total lysates were analyzed by immunoblotting with anti-OTT and HDAC3 antibodies, respectively (*middle* and *bottom panels*).

not shown). To confirm the interaction of OTT with HDAC3 under more physiological conditions, we immunoprecipitated the lysates from HEK293 and MEG-01 cells with anti-HDAC3 antibody, and then co-immunoprecipitated OTT was detected with anti-OTT antibody. Anti-HDAC3, but not control antibody efficiently co-immunoprecipitated endogenous OTT (Fig. 5*B*). Collectively, these results indicate that OTT physically interacts with HDAC3 *in vivo*.

It is well known that HDAC3 is a component of a large nuclear corepressor complex including Sin3A, N-CoR, and SMRT. We next tried to detect interaction of OTT with Sin3A, N-CoR, and SMRT; however, under our experimental conditions, we could not detect direct interaction of OTT with either of them (data not shown). Therefore, future study will be required to address whether OTT might be a component of the nuclear corepressor complex.

Domain Mapping of OTT and HDAC3 for Their Interaction—We next delineated the regions of HDAC3 and OTT responsible for their interaction. Co-immunoprecipitation experiments using deletion mutants of HDAC3 revealed that N-terminal 307 amino acids were sufficient for binding to OTT (Fig. 6, *A* and *B*). Because the expression levels of HDAC3ΔN were consistently very low because of an increase in sensitivity to degradation of the transfected HDAC3ΔN in the cells, we could not formally exclude the possibility that HDAC3ΔN may also mediate the interaction of HDAC3 with OTT.

To determine the binding region of OTT to HDAC3, we constructed a series of deletion mutants of OTT and expressed them as fusion proteins with the DNA-binding domain of GAL4 (Fig. 6*C*). Although a region containing 609–730 amino acids could not bind to HDAC3, the N-terminal region containing three RNA recognition motifs and the C-terminal SPOC domains independently bound to HDAC3 (Fig. 6*D*), indicating that OTT interacts with HDAC3 via multiple regions.

OTT-BSAC Does Not Interact with HDAC3—We next investigated whether BSAC fusion to OTT could affect the ability to

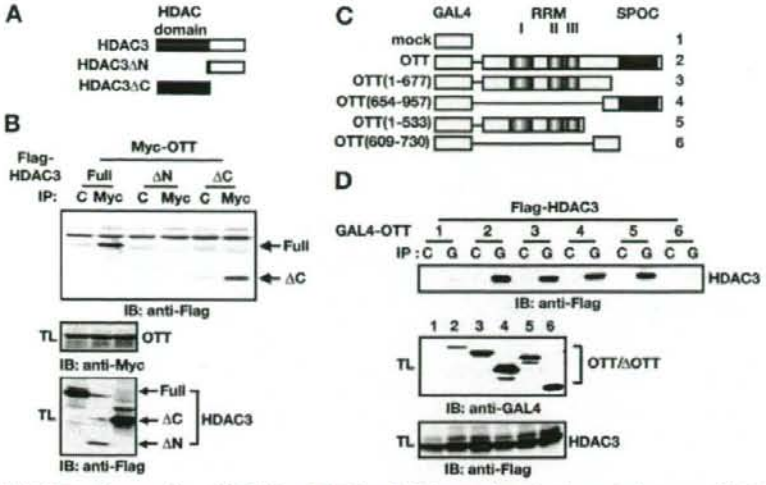

FIGURE 6. **Domain mapping of HDAC3 and OTT for their interaction.** *A*, schematic diagrams of deletion mutants of HDAC3. *B*, N-terminal HDAC domain is responsible for the binding to OTT. HEK293 cells were transfected with the indicated mutants of HDAC3 along with Myc-OTT. After immunoprecipitation (*IP*) with control (*lane C*) or anti-Myc antibodies, co-immunoprecipitated proteins were detected by immunoblotting (*IB*) with anti-FLAG antibody (*top panel*). Expression levels of transfected proteins (*TL*) were analyzed as in Fig. 5*A* (*middle* and *bottom panels*). *C*, schematic diagrams of deletion mutants of OTT fused to the DNA-binding domain of GAL4. *D*, OTT interacts with HDAC3 via multiple regions. HEK293 cells were transfected with the indicated mutants of GAL4-OTT along with FLAG-HDAC3. After immunoprecipitation with control (*lanes C*) or anti-GAL4 (*lanes G*) antibodies, co-immunoprecipitated proteins were detected by immunoblotting with anti-FLAG antibody (*top panel*). Expression levels of transfected proteins (*TL*) were analyzed as in Fig. 5*A* (*middle* and *bottom panels*). The *numbers* indicate each mutant of GAL4-OTT described as in *C*.

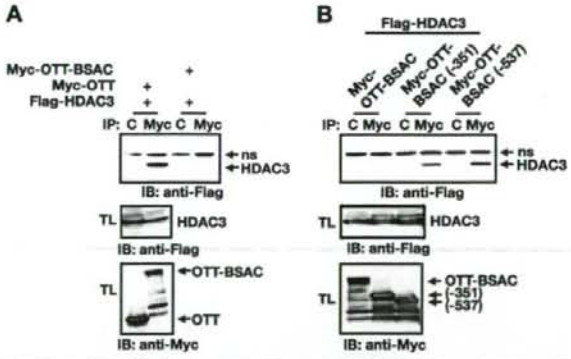

FIGURE 7. **BSAC fusion to OTT disrupts the interaction of OTT with HDAC3.** *A*, HEK293 cells were transfected with FLAG-HDAC3 along with Myc-OTT or Myc-OTT-BSAC. After immunoprecipitation (*IP*) with control (*lane C*) or anti-Myc antibodies, co-immunoprecipitated proteins were detected by immunoblotting (*IB*) with anti-FLAG antibody (*top panel*). Expression levels of the transfected proteins in the total lysates (*TL*) were analyzed as in Fig. 5*A* (*middle* and *bottom panels*). *ns* indicates nonspecific bands. *B*, HEK293 cells were transfected with FLAG-HDAC3 along with the indicated deletion mutants of Myc-OTT-BSAC. Immunoprecipitation and Western blotting were performed as in Fig. 5*A*.

interact with HDAC3. Interestingly, OTT-BSAC lost the ability to interact with HDAC3 (Fig. 7*A*). Given that the domain structure of OTT is preserved in OTT-BSAC, this suggests that some region of BSAC could inhibit the interaction of OTT with HDAC3. To determine the inhibitory region, we constructed C-terminal deletion mutants of OTT-BSAC (Fig. 7*B*). Deletion of C-terminal 351 amino acids containing the TA domain of OTT-BSAC restored the binding to HDAC3, suggesting that the C-terminal TA domain inhibits the binding of HDAC3 to OTT.

DISCUSSION

In the present study, we have shown that a fusion protein OTT-BSAC exhibited strong transcriptional activity to various promoters containing the YY1-binding sequences. Although BSAC predominantly localized in the cytoplasm, OTT-BSAC exclusively localized in the nucleus. This signal-independent nuclear accumulation of OTT-BSAC might contribute to a significant enhancement of transcriptional activity. Moreover, OTT interacted with HDAC3, but this interaction was abolished in OTT-BSAC. Given that OTT negatively regulates the myeloid and megakaryocyte expansion (26, 27), the loss of suppressor function of OTT along with aberrant up-regulation of BSAC-dependent transactivation caused by the fusion may culminate in the development of leukemia.

We and others have previously reported that BSAC activates the promoters containing CArG boxes through association with SRF (9–11). However, given that CArG boxes are found in the promoters of many immediate early genes or muscle-specific genes, it is unlikely that CArG box-dependent transcriptional activity of BSAC directly links to the development of leukemia. Thus, we surmised that OTT-BSAC activates a promoter containing a sequence other than the CArG box(es). We found that OTT-BSAC activated the *GPVI* promoter through YY1-binding sequences. This conclusion is supported by the following results. First, OTT-BSAC-mediated transcriptional activity was abolished on the *GPVI* promoters, in which the YY1-binding sequences were mutated (Fig. 2*B*). Second, YY1 bound to this site using EMSAs (Fig. 2*C*). Third, ChIP assays revealed that endogenous YY1 bound to the *GPVI* promoter (Fig. 2*D*). However, we could not detect the recruitment of transfected OTT-BSAC to the promoter of *GPVI* using ChIP assays under our experimental conditions (Fig. 2*E*). It is reasonable to speculate that only small populations of transfected OTT-BSAC might be recruited to the promoter; therefore such recruitment might be under the detection levels.

Although the present study has shown that OTT-BSAC activates the *GPVI* and other promoters containing the YY1-binding sequences, it remains unclear which transcriptional factor(s) is essential for OTT-BSAC-mediated transcriptional activation. Although overexpression of YY1 attenuated OTT-BSAC-dependent transcriptional activation (Fig. 3*A*), knockdown of YY1 using siRNA did not impair its transcriptional activity (Fig. 3*D*). Given that we could not detect the interaction of YY1 with OTT-BSAC (data not shown), OTT-BSAC might

be recruited to the YY1-binding motif through interaction with a transcription factor other than YY1. Intriguingly, YY2, a member of the YY1 family, has been shown to bind to the consensus binding sequences similar to YY1 (28); YY2 may recruit OTT-BSAC to the *GPVI* promoter. Further study will be required to address this possibility.

A previous study has shown that persistent expression of YY1 in 3DO cells after differentiation signal could perturb the granulocyte differentiation (18). Moreover, up-regulation of *YY1* mRNA is frequently observed in some patients of acute myeloid leukemia (18). These results indicate an intimate link between deregulation of YY1 and leukemia. Together, OTT-BSAC might modulate YY1- and/or YY1-related transcriptional factor-dependent transcription, culminating in the development of leukemia.

Another important finding of this study is that OTT fusion to the N terminus of BSAC resulted in signal-independent nuclear accumulation of OTT-BSAC. A previous study has shown that nuclear translocation of BSAC is tightly regulated by the Rho-actin signaling pathway (12). Consistently, under unstimulated conditions, endogenous BSAC predominantly localized in the cytoplasm (Fig. 4). These results suggest that transcriptional activity of BSAC is at least partly regulated by its subcellular localization. This might well explain the reason why OTT-BSAC shows stronger transcriptional activity than BSAC. However, the mechanism by which OTT-BSAC constitutively accumulates in the nucleus remains to be solved in this study. One possible scenario is that the nuclear localization signal(s) of OTT might dominate over the cytoplasmic retention signal(s) of BSAC. Although BSAC has its own nuclear localization signals in the basic domain, N-terminal RPEL motifs are considered to sequestrate BSAC to the cytoplasm via interaction with G actin under unstimulated conditions (12). Therefore, OTT might disrupt such inhibition, resulting in constitutive nuclear translocation of OTT-BSAC.

A recent study has shown that deletion of *OTT* gene results in megakaryocytic expansion (27). In addition, knockdown of *OTT/RBM15* gene using RNA interference promotes myeloid differentiation (26), suggesting an inhibitory role for OTT in myeloid and megakaryocyte development. These results are consistent with our present study, in which OTT might act as a transcriptional repressor via interaction with HDAC3 (Fig. 6). Given that this transcriptional repressor activity of OTT might be abolished in OTT-BSAC, the loss of OTT-mediated suppressor function of OTT-BSAC along with aberrant up-regulation of BSAC-dependent transcriptional activity might synergistically contribute to the development of leukemia.

Acknowledgments—We thank Drs. Don Ayer, Edward Seto, Stuart Schreiber, Jiemin Wang, A. Gregory Materal, Ron M. Evans, the Kazusa DNA Institute, Takeyuki Sato, and Masao Seto for providing reagents and cell lines. We also thank Drs. Alan B. Cantor, Jean-Pierre Bourquin, Yuriko Suzuki, Tatsuo Fukagawa, Mitsuru Matsumoto, and Mikiko Chihara-Siomi for helpful discussion.

REFERENCES

1. Struhl, K. (1998) *Genes Dev.* **12,** 599–606
2. Ng, H. H., and Bird, A. (2000) *Trends Biochem. Sci* **25,** 121–126
3. Yang, X. J., and Gregoire, S. (2005) *Mol. Cell. Biol.* **25,** 2873–2884
4. Jepsen, K., and Rosenfeld, M. G. (2002) *J. Cell Sci.* **115,** 689–698
5. Shi, Y., Downes, M., Xie, W., Kao, H. Y., Ordentlich, P., Tsai, C. C., Hon, M., and Evans, R. M. (2001) *Genes Dev.* **15,** 1140–1151
6. Ariyoshi, M., and Schwabe, J. W. (2003) *Genes Dev.* **17,** 1909–1920
7. Mercher, T., Coniat, M. B., Monni, R., Mauchauffe, M., Khac, F. N., Gressin, L., Mugneret, F., Leblanc, T., Dastugue, N., Berger, R., and Bernard, O. A. (2001) *Proc. Natl. Acad. Sci. U. S. A.* **98,** 5776–5779
8. Ma, Z., Morris, S. W., Valentine, V., Li, M., Herbrick, J. A., Cui, X., Bouman, D., Li, Y., Mehta, P. K., Nizetic, D., Kaneko, Y., Chan, G. C., Chan, L. C., Squire, J., Scherer, S. W., and Hitzler, J. K. (2001) *Nat. Genet.* **28,** 220–221
9. Sasazuki, T., Sawada, T., Sakon, S., Kitamura, T., Kishi, T., Okazaki, T., Katano, M., Tanaka, M., Watanabe, M., Yagita, H., Okumura, K., and Nakano, H. (2002) *J. Biol. Chem.* **277,** 28853–28860
10. Wang, D. Z., Li, S., Hockemeyer, D., Sutherland, L., Wang, Z., Schratt, G., Richardson, J. A., Nordheim, A., and Olson, E. N. (2002) *Proc. Natl. Acad. Sci. U. S. A.* **99,** 14855–14860
11. Cen, B., Selvaraj, A., Burgess, R. C., Hitzler, J. K., Ma, Z., Morris, S. W., and Prywes, R. (2003) *Mol. Cell. Biol.* **23,** 6597–6608
12. Miralles, F., Posern, G., Zaromytidou, A. I., and Treisman, R. (2003) *Cell* **113,** 329–342
13. Li, S., Chang, S., Qi, X., Richardson, J. A., and Olson, E. N. (2006) *Mol. Cell. Biol.* **26,** 5797–5808
14. Sun, Y., Boyd, K., Xu, W., Ma, J., Jackson, C. W., Fu, A., Shillingford, J. M., Robinson, G. W., Hennighausen, L., Hitzler, J. K., Ma, Z., and Morris, S. W. (2006) *Mol. Cell. Biol.* **26,** 5809–5826
15. Shi, Y., Lee, J. S., and Galvin, K. M. (1997) *Biochim. Biophys. Acta* **1332,** 49–66
16. Thomas, M. J., and Seto, E. (1999) *Gene (Amst.)* **236,** 197–208
17. Donohoe, M. E., Zhang, X., McGinnis, L., Biggers, J., Li, E., and Shi, Y. (1999) *Mol. Cell. Biol.* **19,** 7237–7244
18. Erkeland, S. J., Valkhof, M., Heijmans-Antonissen, C., Delwel, R., Valk, P. J., Hermans, M. H., and Touw, I. P. (2003) *Blood* **101,** 1111–1117
19. Ogura, M., Morishima, Y., Ohno, R., Kato, Y., Hirabayashi, N., Nagura, H., and Saito, H. (1985) *Blood* **66,** 1384–1392
20. Nishiyama, C., Hasegawa, M., Nishiyama, M., Takahashi, K., Akizawa, Y., Yokota, T., Okumura, K., Ogawa, H., and Ra, C. (2002) *J. Immunol.* **168,** 4546–4552
21. Muraoka, O., Kaisho, T., Tanabe, M., and Hirano, T. (1993) *Immunol. Lett.* **37,** 159–165
22. Nakano, H., Shindo, M., Sakon, S., Nishinaka, S., Mihara, M., Yagita, H., and Okumura, K. (1998) *Proc. Natl. Acad. Sci. U. S. A.* **95,** 3537–3542
23. Kanada, S., Nakano, N., Potaczek, D. P., Maeda, K., Shimokawa, N., Niwa, Y., Fukai, T., Sanak, M., Szczeklik, A., Yagita, H., Okumura, K., Ogawa, H., and Nishiyama, C. (2008) *J. Immunol.* **180,** 8204–8210
24. Holmes, M. L., Bartle, N., Eisbacher, M., and Chong, B. H. (2002) *J. Biol. Chem.* **277,** 48333–48341
25. Wang, D., Chang, P. S., Wang, Z., Sutherland, L., Richardson, J. A., Small, E., Krieg, P. A., and Olson, E. N. (2001) *Cell* **105,** 851–862
26. Ma, X., Renda, M. J., Wang, L., Cheng, E. C., Niu, C., Morris, S. W., Chi, A. S., and Krause, D. S. (2007) *Mol. Cell. Biol.* **27,** 3056–3064
27. Raffel, G. D., Mercher, T., Shigematsu, H., Williams, I. R., Cullen, D. E., Akashi, K., Bernard, O. A., and Gilliland, D. G. (2007) *Proc. Natl. Acad. Sci. U. S. A.* **104,** 6001–6006
28. Nguyen, N., Zhang, X., Olashaw, N., and Seto, E. (2004) *J. Biol. Chem.* **279,** 25927–25934

European Journal of Haematology ISSN 0902-4441

CASE REPORT

A complex t(1;22;11)(q44;q13;q23) translocation causing *MLL-p300* fusion gene in therapy-related acute myeloid leukemia

Hiroaki Ohnishi[1], Tomohiko Taki[2], Hiroshi Yoshino[3], Junko Takita[4], Kohmei Ida[5], Masami Ishii[3], Kazuhiro Nishida[6], Yasuhide Hayashi[7], Masafumi Taniwaki[6], Fumio Bessho[3], Takashi Watanabe[1]

[1]Department of Laboratory Medicine, Kyorin University, Tokyo, Japan; [2]Department of Molecular Laboratory Medicine, Kyoto Prefectural University of Medicine, Graduate School of Medical Science, Kyoto, Japan; [3]Department of Pediatrics, Kyorin University, Tokyo, Japan; [4]Department of Pediatrics and Cell Therapy and Transplantation Medicine, Tokyo University, Tokyo, Japan; [5]Department of Pediatrics, Tokyo University, Tokyo, Japan; [6]Department of Molecular Hematology and Oncology, Kyoto Prefectural University of Medicine, Graduate School of Medical Science, Kyoto, Japan; [7]Gunma Children's Medical Center, Gunma, Japan

Abstract

The p300 protein shows a striking homology with cyclic-AMP-response-element-binding-protein binding protein (CBP) and both proteins form a family of DNA-binding transcriptional coactivators/histone acetyltransferases. The authors, herein, report a therapy-related acute myeloid leukemia with *MLL-p300* fusion gene. Spectral karyotyping clarified that chromosome 11 is involved in complex t(1;22;11)(q44;q13;q23), and is fused to the chromosome 22, and direct sequencing revealed the fusion of exon 8 of *MLL* and exon 15 of *p300* in this case. This is only the second reported case of leukemia with an *MLL-p300* fusion gene, and the other case with *MLL-p300* was also a therapy-related leukemia. Considering that the *MLL-CBP* fusion gene is also found almost exclusively in therapy-related leukemia, the association of *MLL-p300* and *MLL-CBP* with therapy-related leukemia rather than *de novo* leukemia is thereby suggested.

Key words *MLL*; *p300*; acute myeloid leukemia; therapy-related leukemia; spectral karyotyping

Correspondence Dr Hiroaki Ohnishi, Department of Laboratory Medicine, Kyorin University 6-20-2, Shinkawa, Mitaka, Tokyo 181-8611, Japan. Tel: +81 (422) 47 5511; Fax: +81 (422) 79 3471; e-mail: onishi@ks.kyorin-u.ac.jp

Accepted for publication 29 August 2008

doi:10.1111/j.1600-0609.2008.01154.x

The 11q23 translocations are frequent in hematological malignancies, occurring in both childhood (approximately 10%) and adult (approximately 5%) acute leukemias, and in most patients with therapy-related leukemia induced by topoisomerase II inhibitors (1). The *MLL* gene is rearranged as a consequence of 11q23 translocation, and at least 60 partner genes for *MLL* have so far been identified (2).

p300, which was originally cloned as a nuclear binding target of the adenovirus E1A oncoprotein, forms a family with cyclic-AMP-response-element-binding-protein (CREB) binding protein (CBP) (3). Both *p300/EP300* and *CBP* encode histone acetyltransferases (HAT) which regulate transcription via chromatin remodeling and are important in the processes of cell proliferation and differentiation (4–6). The mutation and translocation of *p300* and *CBP* genes have been observed in a subset of tumors and hematological malignancies, respectively, thus suggesting the involvement of these genes in the development of human cancer (4–6). We have previously reported the *p300* gene to be fused to the *MLL* gene in a case of therapy-related acute myeloid leukemia (AML) with t(11;22)(q23;q13) (7). Previous studies also revealed that *CBP* forms a fusion gene with *MLL* in AML, and all but one of the reported cases was therapy-related AML (8–12). These results imply that the *MLL-p300* and *MLL-CBP* fusion genes are associated with the development of therapy-related leukemia rather than with *de novo* leukemia. Nevertheless, this association has not been confirmed in *MLL-p300* because no other case with the *MLL-p300* fusion gene has been reported to date. We herein report

a second case of therapy-related AML with *MLL-p300*, which further suggests the association of this fusion gene with therapy-related leukemia.

Case report

A 5-yr-old girl was admitted to our hospital because of a continuous fever and petechiae. She had been diagnosed with neuroblastoma at the age of 2, and treated by an operation followed by 6 months of chemotherapy including pirarubicin, carboplatinum and cyclophosphamide. On admission, she presented with lymphadenopathy but no hepatosplenomegaly. The peripheral blood data were hemoglobin 51 g/L, platelet 7.0×10^9/L and white blood cells 5.1×10^9/L (blasts 2.5%). The diagnosis from the bone marrow aspirate was AML M1 according to the French-American-British classification or AML without maturation according to the WHO classification. Immunophenotyping by CD45 gating revealed the blast cells to be positive for CD4, 7, 13, 19, 33, 34 and human leukocyte antigen (HLA)-DR but negative for CD3, 41 and glycophorin A. She was treated by two courses of chemotherapy followed by cord blood transplantation from an unrelated donor. She is presently alive and free of leukemia and neuroblastoma at 1 yr after transplantation.

Materials and methods

Karyotyping

Regular G-banding karyotyping of the leukemic cells was performed according to previously described protocols. A spectral karyotyping (SKY) was carried out with a SkyPaint kit (Applied Spectral Imaging, Migdal Ha'Emek, Israel) (13). The signal detection was performed according to the manufacturer's instructions.

Southern blot analysis

High-molecular-weight DNA was extracted from the bone marrow samples obtained at the diagnosis of AML, and 10 mg of DNA was analyzed as reported previously (14). A 0.9-kb MLL cDNA probe and restriction enzymes *Bam*HI and *Hind*III were used.

Reverse transcriptase-polymerase chain reaction (RT-PCR) and direct sequence analysis

The total RNA was extracted from the bone marrow samples obtained at the diagnosis of AML, and reverse-transcribed to cDNA as previously described (7). The primers used to amplify the *MLL-p300* fusion transcripts were as follows: MLL-7S: TCCTCAGCACTCTCTCCAA (within exon 7 of *MLL*), MLL-9S: GGTGTTGTCGTCGTTGCAAA (within exon 9 of *MLL*), p300-7.5A: GCTGAAGTACTTGGCTGGTC (within exon 16 of *p300*) and p300-8A: GGCTCCTGATACTGTCCAGT (within exon 18 of *p300*). The *MLL* exon numbering system proposed by Rasio *et al.* (15) was utilized in this study. The positive bands were cut out from the agarose gel and subjected to a direct sequencing analysis using the same primers described above.

Fluorescence *in situ* hybridization (FISH)

A FISH analysis of the *p300* gene was performed according to the previously described protocols using the probes RP11-188A17 and RP11-107O11 (16).

Results

A chromosomal analysis of the blast cells by the G-banding method showed 46,XX,t(1;11)(q44;q23),t(10;17)(q22;q21) in 20 out of the 20 investigated cells (Fig. 1A), and all these abnormalities disappeared in the bone marrow cells at the remission. A Southern blot analysis of the blast DNA revealed rearrangement of the *MLL* gene (data not shown). Because of the complex karyotype, we performed a SKY to confirm the result of the chromosomal analysis. The SKY demonstrated that chromosome 11 was actually involved in complex t(1;22;11)(q44;q13;q23), and the centromeric region of chromosome band 11q23 was fused to the chromosome 22 instead of the chromosome 1 (Fig. 1B). Previously, two genes, *CDCREL1* at 22q11.2 and *p300* at 22q13, were reported to be involved as translocation partners in t(11;22)(q23;q11.2) and t(11;22)(q23;q13), respectively (2). Of these, *p300* was assumed to be closely associated with therapy-related leukemia, because the cases with *MLL-p300* or *MLL-CBP* fusion were mostly therapy-related leukemia, although cases with *MLL-CDCREL1* were not. We therefore conducted RT-PCR in order to detect the *MLL-p300* fusion gene. Two bands (a clear band with slower electrophoresis mobility and a faint band with faster electrophoresis mobility) were detected by PCR with either primer set MLL-7S/p300-7.5A or MLL-7S/p300-8A, although no positive band was detected by the primer sets MLL-9S/p300-7.5A or MLL-9S/p300-8A (Fig. 2A). A direct sequencing of the clear band identified the fusion of exon 8 of *MLL* and exon 15 of *p300* (Fig. 2B). A direct sequencing of the faint band identified the fusion of exon 7 of *MLL* and exon 15 of *p300*, which was considered to be generated by alternative splicing. A FISH using the probes RP11-188A17 and RP11-107O11 confirmed the cleavage of the *p300* gene (Fig. 1C).

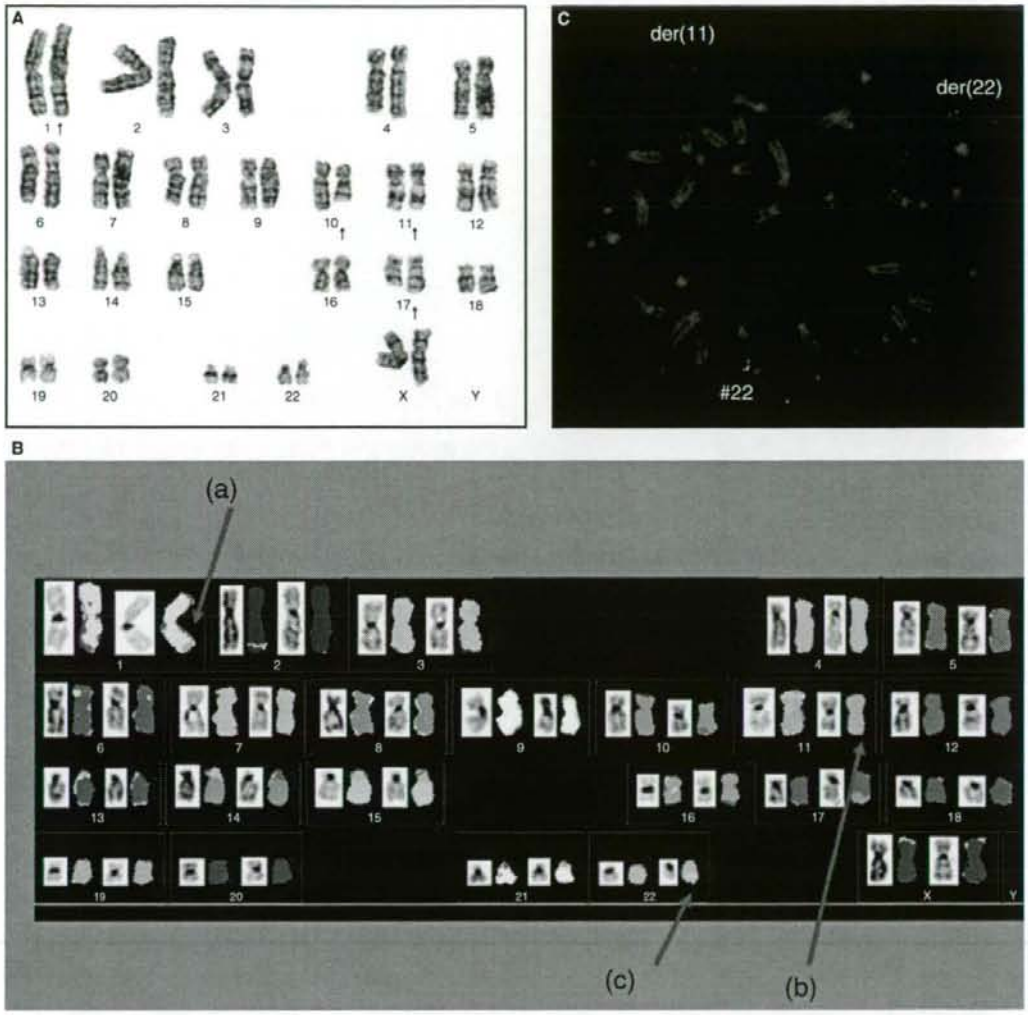

Figure 1 Chromosomal analyses of leukemic cells. (A) Conventional G-banding. Arrows denote the chromosomes assumed to be involved in translocation. (B) Spectral karyotyping. Arrows (a), (b), and (c) indicate der(11q), der(22q), and der(1q), respectively. (C) FISH. Green signals represent the probe RP11-188A17 which binds to the centromeric side of the *p300* gene on chromosome 22. Red signals represent the probe RP11-1078O11 which binds to the telomeric side of the *p300* gene. The split of the both signals, shown as der(11) and der(22), indicates the cleavage of the *p300* gene.

Discussion

This is only the second reported case of leukemia with *MLL-p300* fusion gene. The sole case with *MLL-p300* fusion was previously described by our group, and it was also a therapy-related leukemia following chemotherapy by topoisomerase II inhibitor. In addition, *MLL-CBP* has been detected almost exclusively in cases with therapy-related leukemia following topoisomerase II inhibitor therapy (9). As *p300* and *CBP* represent a striking homology, it is possible that common mechanisms may be involved in the translocation of *p300* or *CBP* to *MLL*. In a previous study, Zhang *et al.* (17) have characterized the genomic breakpoints in six cases of leukemia with *MLL-CBP* fusion. Despite intensive attempts, however, they could not detect any topoisomerase II cleavage sites in the regions surrounding the breakpoints of *MLL* or *CBP*. Several studies analyzing other types of translocation have provided inconsistent results regarding the association of genomic breakpoints and topoisomerase II

Figure 2 Results of (A) RT-PCR and (B) direct sequencing of the fusion gene. (A) Bone marrow cells of the patient at diagnosis (P) and a negative control (C). M: 1-kb marker. A primer set MLL-7S/p300-8A was used. (B) Direct sequencing of the upper band demonstrated fusion of exon 8 of *MLL* and exon 15 of *p300*.

cleavage sites in therapy-related leukemias (17–19). These results suggest that the association of the genomic breakpoints of translocations in therapy-related leukemias and the topoisomerase II cleavage sites is more complicated than has been assumed. Further accumulation of cases with *MLL-p300* and an analysis of the genomic breakpoints may provide insight regarding this issue.

A schematic presentation of the predicted MLL-p300 fusion protein in this case and the previously reported

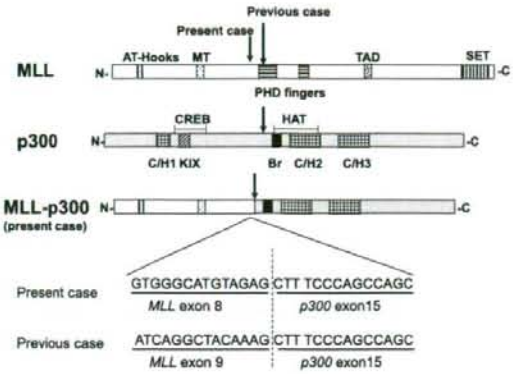

Figure 3 Schematic representation of the predicted MLL-p300 fusion proteins of the present and the previous reported cases. Arrows denote the breakpoints of each gene. MT, methyltransferase; TAD, transactivation domain; CREB, CREB-binding region; HAT, histone acetyltransferase; C/H, cysteine/histidine rich region; Br, bromodomain.

case is shown in Fig. 3. In both cases, the AT-hook, DNA methyltransferase, and a transcriptional repression domain of MLL are retained. However, a part of the plant homeodomain finger domain retained in the chimeric protein in the former case was lacking in the present case, suggesting that this domain is not critical in the development of leukemia in cases with MLL-p300. On the other hand, both chimeric proteins retained the identical part of p300 which includes the HAT domain and the transactivation domain but does not include the CREB-binding region. While MLL-CBP fusion proteins have been reported to retain almost all parts of CBP (9), the CREB-binding region may not be crucial for developing leukemia in cases with MLL-p300 or MLL-CBP fusion. Recent studies suggest that different mechanisms might be involved in the leukemogenesis of MLL fusion proteins, depending on whether the fusion partner is nuclear or cytoplasmic factors (20). The nuclear factors such as CBP and p300 have transcription activity, and this function might be deregulated by fusion with MLL (6). Furthermore, an aberration of other HAT-associated

Table 1 Clinical and biological features of the two cases with *MLL-p300*

	Sex	Age (yr)	Former malignancy	Topoisomerase dose	Latency[1] (month)	Subtype of leukemia	Immunophenotype	Cytogenetics	Fusion gene
Previous case (7)	M	9	Non-Hodgkin lymphoma	Etoposide 5200 mg/m^2	67	AML M1	CD7, 33	48,XY,+8,+8, t(11;22)(q23;q13)	*MLL* exon 9/*p300* exon 15
Present case	F	5	Neuroblastoma	Pirarubicine 300 mg/m^2	36	AML M2	CD4, 7, 13, 19, 33, 34	46,XX,t(1;22;11)(q44;q13;q23)[2], t(10;17)(q22;q21)	*MLL* exon 7 and 8/*p300* exon 15

AML, acute myeloid leukemia.
[1]Latency between the onset of the former malignancy and the secondary leukemia.
[2]Revealed by spectral karyotyping.

genes is also known to be involved in the development of leukemia. For example, *MOZ* or *MORF* is involved in translocation of AML in the forms of *MOZ-CBP*, *MOZ-p300*, *MOZ-TIF2* and *MORF-CBP* (19, 21–23). *TIF2* is also a HAT-associated gene, and all of these translocations retain the HAT domain in involved genes. These results suggest an association of activated transcription by HAT with leukemogenesis in these fusion transcripts. A further functional analysis of these fusion proteins will give insight into the mechanism of leukemogenesis in these cases (Table 1).

SKY was useful for revealing cryptic t(11;22)(q23;q13) in this case. Performing SKY for blast cells is thereby recommended unless a known translocation is detected by conventional G-banding after a diagnosis of leukemia has been made. However, SKY is not always sufficiently informative. In cases where one gene is found to be rearranged but the translocation partner gene is undetectable, other PCR-based methods, such as panhandle PCR or bubble PCR, are also known to be useful in revealing the translocation partner gene (24, 25). The clarification of a cryptic translocation and a fusion gene using these techniques will provide further information regarding the phenotype of leukemia, while it is also helpful in clinical settings, such as when used for the detection of minimal residual disease.

Acknowledgements

We wish to thank Ms Satsuki Matsushima and Ms Yoriko Endo from the Department of Laboratory Medicine at Kyorin University Hospital and Ms Minako Goto from the Department of Molecular Hematology and Oncology at Kyoto Prefectural University of Medicine for their technical assistance.

References

1. Rowley JD. The critical role of chromosome translocations in human leukemias. *Annu Rev Genet* 1998;**32**:495–519.
2. Meyer C, Schneider B, Jakob S, *et al.* The MLL recombinome of acute leukemias. *Leukemia* 2006;**20**:777–84.
3. Arany Z, Newsome D, Oldread E, Livingston DM, Eckner R. A family of transcriptional adaptor proteins targeted by the E1A oncoprotein. *Nature* 1995;**374**:81–4.
4. Gayther SA, Batley SJ, Linger L, *et al.* Mutations truncating the EP300 acetylase in human cancers. *Nat Genet* 2000;**24**:300–3.
5. Iyer NG, Ozdag H, Caldas C. p300/CBP and cancer. *Oncogene* 2004;**23**:4225–31.
6. Chan HM, La Thangue NB. p300/CBP proteins: HATs for transcriptional bridges and scaffolds. *J Cell Sci* 2001;**114**:2363–73.
7. Ida K, Kitabayashi I, Taki T, Taniwaki M, Noro K, Yamamoto M, Ohki M, Hayashi Y. Adenoviral E1A-associated protein p300 is involved in acute myeloid leukemia with t(11;22)(q23;q13). *Blood* 1997;**90**:4699–704.
8. Taki T, Sako M, Tsuchida M, Hayashi Y. The t(11;16)(q23;p13) translocation in myelodysplastic syndrome fuses the MLL gene to the CBP gene. *Blood* 1997;**89**:3945–50.
9. Rowley JD, Reshmi S, Sobulo O, *et al.* All patients with the t(11;16)(q23;p13.3) that involves MLL and CBP have treatment-related hematologic disorders. *Blood* 1997;**90**:535–41.
10. Sobulo OM, Borrow J, Tomek R, Reshmi S, Harden A, Schlegelberger B, Housman D, Doggett NA, Rowley JD, Zeleznik-Le NJ. MLL is fused to CBP, a histone acetyltransferase, in therapy-related acute myeloid leukemia with a t(11;16)(q23;p13.3). *Proc Natl Acad Sci USA* 1997;**94**:8732–7.
11. Satake N, Ishida Y, Otoh Y, Hinohara S, Kobayashi H, Sakashita A, Maseki N, Kaneko Y. Novel MLL-CBP fusion transcript in therapy-related chronic myelomonocytic leukemia with a t(11;16)(q23;p13) chromosome translocation. *Genes Chromosomes Cancer* 1997;**20**:60–3.
12. Sugita K, Taki T, Hayashi Y, Shimaoka H, Kumazaki H, Inoue H, Konno Y, Taniwaki M, Kurosawa H, Eguchi M. MLL-CBP fusion transcript in a therapy-related acute myeloid leukemia with the t(11;16)(q23;p13) which developed in an acute lymphoblastic leukemia patient with Fanconi anemia. *Genes Chromosomes Cancer* 2000;**27**:264–9.
13. Taki T, Akiyama M, Saito S, Ono R, Taniwaki M, Kato Y, Yuza Y, Eto Y, Hayashi Y. The MYO1F, unconventional myosin type 1F, gene is fused to MLL in infant acute monocytic leukemia with a complex translocation involving chromosomes 7, 11, 19 and 22. *Oncogene* 2005;**24**:5191–7.
14. Ono R, Taki T, Taketani T, Kawaguchi H, Taniwaki M, Okamura T, Kawa K, Hanada R, Kobayashi M, Hayashi Y. SEPTIN6, a human homologue to mouse Septin6, is fused to MLL in infant acute myeloid leukemia with complex chromosomal abnormalities involving 11q23 and Xq24. *Cancer Res* 2002;**62**:333–7.
15. Rasio D, Schichman SA, Negrini M, Canaani E, Croce CM. Complete exon structure of the ALL1 gene. *Cancer Res* 1996;**56**:1766–9.
16. Nomura K, Kanda-Akano Y, Shimizu D, *et al.* An additional segment at 1p36 derived from der(18)t(14;18) in patients with diffuse large B-cell lymphomas transformed from follicular lymphoma. *Ann Hematol* 2005;**84**:474–6.
17. Zhang Y, Zeleznik-Le N, Emmanuel N, *et al.* Characterization of genomic breakpoints in MLL and CBP in leukemia patients with t(11;16). *Genes Chromosomes Cancer* 2004;**41**:257–65.
18. Langer T, Metzler M, Reinhardt D, *et al.* Analysis of t(9;11) chromosomal breakpoint sequences in childhood

acute leukemia: almost identical MLL breakpoints in therapy-related AML after treatment without etoposides. *Genes Chromosomes Cancer* 2003;**36**:393–401.

19. Panagopoulos I, Fioretos T, Isaksson M, Samuelsson U, Billström R, Strömbeck B, Mitelman F, Johansson B. Fusion of the MORF and CBP genes in acute myeloid leukemia with the t(10;16)(q22;p13). *Hum Mol Genet* 2001;**10**:395–404.
20. Li ZY, Liu DP, Liang CC. New insight into the molecular mechanisms of MLL-associated leukemia. *Leukemia* 2005;**19**:183–90.
21. Borrow J, Stanton VP Jr, Andresen JM, *et al.* The translocation t(8;16)(p11;p13) of acute myeloid leukaemia fuses a putative acetyltransferase to the CREB-binding protein. *Nat Genet* 1996;**14**:33–41.
22. Chaffanet M, Gressin L, Preudhomme C, Soenen-Cornu V, Birnbaum D, Pébusque MJ. MOZ is fused to p300 in an acute monocytic leukemia with t(8;22). *Genes Chromosomes Cancer* 2000;**28**:138–44.
23. Carapeti M, Aguiar RC, Goldman JM, Cross NC. A novel fusion between MOZ and the nuclear receptor coactivator TIF2 in acute myeloid leukemia. *Blood* 1998;**91**:3127–33.
24. Suzukawa K, Shimizu S, Nemoto N, Takei N, Taki T, Nagasawa T. Identification of a chromosomal breakpoint and detection of a novel form of an MLL-AF17 fusion transcript in acute monocytic leukemia with t(11;17)(q23;q21). *Int J Hematol* 2005;**82**:38–41.
25. Zhang JG, Goldman JM, Cross NC. Characterization of genomic BCR-ABL breakpoints in chronic myeloid leukaemia by PCR. *Br J Haematol* 1995;**90**:138–46.

ELSEVIER

Cancer Genetics and Cytogenetics 188 (2009) 99–102

CANCER GENETICS AND CYTOGENETICS

Short communication

Transient abnormal myelopoiesis in a Down syndrome newborn followed by acute myeloid leukemia: identification of the same chromosomal abnormality in both stages

Toshiyuki Kitoh[a,b,*], Tomohiko Taki[c], Yasuhide Hayashi[d], Kenji Nakamura[e], Tamotsu Irino[b,f], Mitsuhiko Osaka[f]

[a]*Department of Hematology/Oncology, Shiga Medical Center for Children, 5-7-30 Moriyama, Moriyama 524-0022, Moriyama, Japan*
[b]*Department of Laboratory Medicine, Shiga Medical Center for Children, Moriyama, Japan*
[c]*Department of Molecular Laboratory Medicine, Kyoto Prefectural University of Medicine Graduate School of Medical Science, Kyoto, Japan*
[d]*Gunma Children's Medical Center, Gunma, Japan*
[e]*Department of Pediatrics, Otsu Red Cross Hospital, Otsu, Japan*
[f]*Division of Cancer Research, Shiga Medical Center Research Institute, Moriyama, Japan*

Received 18 June 2008; received in revised form 31 July 2008; accepted 13 August 2008

Abstract A transient abnormal myelopoiesis was observed in a newborn with Down syndrome. Cytogenetic study revealed multiple oligoclonal abnormalities: 47,XY,inv(6)(p23q21),+21c[3]/47,XY, der(7)t(1;7)(q25;p15),+21c[1]/47,XY,del(13)(q?),+21c[1]/47,XY,+21c[15]. Ten months after the patient achieved remission, the transient abnormal myelopoiesis evolved to an acute megakaryoblastic leukemia. Cytogenetic study revealed only a single clonal abnormality, 47,XY,der(7)t(1;7)(q25;p15),+21c, identical to one of the structural changes seen at birth. Sequence analysis of the *GATA1* gene revealed a deletion–insertion mutation within the exon 2 introducing a stop codon after Arg 64. It may be that the der(7)t(1;7)(q25;p15) abnormality played some selective role in the development of acute megakaryoblastic leukemia in this patient. To our knowledge, the present case is unique in demonstrating a subclone with der(7)t(1;7)(q25;p15) evolving to acute leukemia.

1. Introduction

Approximately 10% of patients with Down syndrome are born with transient abnormal myelopoiesis (TAM) [1,2]. Of these cases, ~20% recur as acute megakaryoblastic leukemia (AMKL) [3]. Acquired mutations in *GATA1* in the leukemic blasts are detected in virtually all of these cases [4–7], but the second hit for the full expression of AMKL is still a matter of discussion [6,7]. GATA1 is a transcription factor that regulates megakaryocytic differentiation, and the mutations observed are considered to cause accumulation of poorly differentiated megakaryocytic precursors [4]. Strikingly, *GATA1* is located on chromosome X; therefore, genetic interaction of *GATA1* with one or more genes on other chromosomes presumably contributes to the development of AMKL in Down syndrome.

Acute myeloid leukemia (AML) and myelodysplastic syndrome (MDS) in Down syndrome often demonstrate chromosomal abnormalities in addition to the constitutional trisomy 21 [8–12]. These include both numerical and structural abnormalities, mostly complete or partial trisomy of a specific chromosome; reciprocal translocations are relatively rare. The role of these chromosomal translocations in developing leukemia in Down syndrome is also unknown. Here, we report the case of a Down syndrome patient who developed AMKL showing der(7)t(1;7)(q25;p15) following TAM at birth.

2. Case report

This Down syndrome patient was a boy born at 39 weeks gestational age, weighing 3,235 g. Thrombocytopenia was revealed after birth. At 5 days after birth, he was diagnosed as having TAM. Initial white blood cell count was 13,200/μL with 7% blasts, hemoglobin was 15.0 g/dL, and platelet count was 52,000/μL. Chromosomal analysis of bone marrow cells at diagnosis revealed the

* Corresponding author. Tel.: +81-77-582-6200; fax: +81-77-582-6304. (T. Kitoh).
E-mail address: tkitoh-mccs@umin.ac.jp (T. Kitoh).

0165-4608/09/$ – see front matter
doi:10.1016/j.cancergencyto.2008.08.011

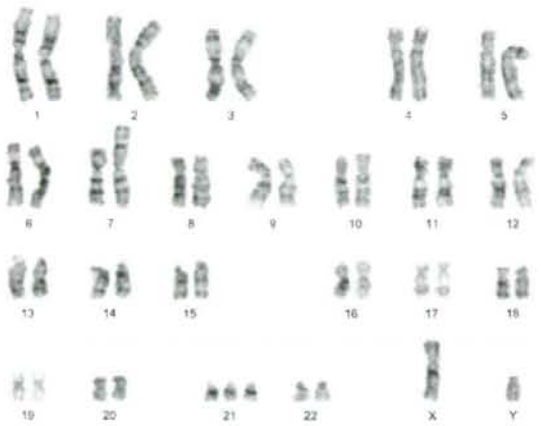

Fig. 1. Karyogram of the blast in leukemic phase showing 47,XY,der(7)t(1;7)(q25;p15),+21c.

karyotype 47,XY,inv(6)(p23q21),+21c[3]/47,XY,der(7)t(1;7)(q25;p15),+21c[1]/47,XY,del(13)(q?),+21c[1]/47,XY,+21c[15]/. Although he was not treated, his white blood cell count gradually decreased within 2 months, and at 7 months after birth his platelet count spontaneously recovered to within the normal range (although he suffered from thrombocytopenia due to an unknown viral infection). At 10 months after birth, the blasts increased suddenly.

Persistent thrombocytopenia was noted after platelet transfusions twice weekly. A bone marrow aspirate showed excessive myelofibrosis. Immunophenotyping of peripheral blasts showed $CD7^+$, $CD13^+$, $CD33^+$, $CD38^+$, $CD41^+$, $CD42b^+$, $CD56^+$, $CD157^+$, and HLA-DR^+. Chromosome analysis showed a der(7)t(1;7)(q25;p15) abnormality, in addition to the constitutional trisomy 21 (Fig. 1). Spectral karyotyping further confirmed the presence of the t(1;7) translocation, expressed as 47,XY,der(7)t(1;7)(q25;p15),+21c (Fig. 2), resulting in partial trisomy of 1q.

We analyzed the *GATA1* mutation in the peripheral blood sample, after written informed consent was obtained from his parents. Genomic DNA was extracted, and then polymerase chain reaction (PCR) was performed. Subcloning and nucleotide sequencing of PCR products were performed as described previously [6]. Sequence analysis of *GATA1* gene revealed a deletion–insertion mutation within exon 2, introducing premature stop codon after Arg 64 (Fig. 3).

A trephine biopsy revealed the presence of a typical megakaryocyte proliferation and prominent fibrosis. The final diagnosis of AMKL led to the initiation of combination therapy of pirarubicin HCl (25 mg/m^2 per day for 2 days), cytosine arabinoside (100 mg/m^2 per day for 7 days), and etoposide (150 mg/m^2 per day for 3 days) [13]. Complete remission was achieved after two courses of the therapy. Continuation of the consolidation therapy was uneventful, and six cycles of the same regimen were completed. As of writing, the patient had been in continuous complete remission without marked side effects for 5 years after initiation of the therapy.

3. Discussion

Recent collaborative studies on AML in Down syndrome children have established that the most frequent cytogenetic abnormality in AML or MDS in Down syndrome is trisomy 8 or partial trisomy of 1q [2,14–17]. Because AML and MDS with Down syndrome have distinct biologic and clinical features, the identification of Down syndrome patients with a mild or normal phenotype in the AML/MDS population is of fundamental importance for clinical diagnosis and management. Partial trisomy of 1q

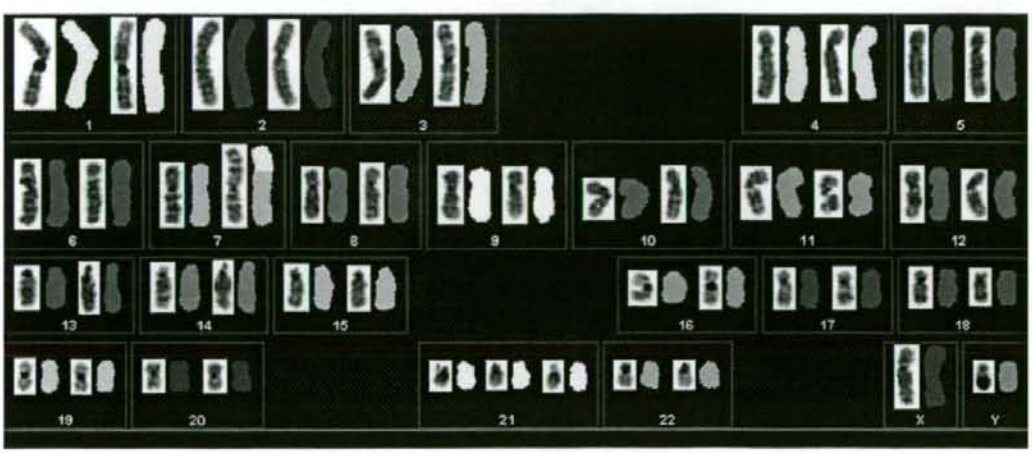

Fig. 2. Spectral karyotyping showing 47,XY,der(7)t(1;7)(q25;p15),+21c.

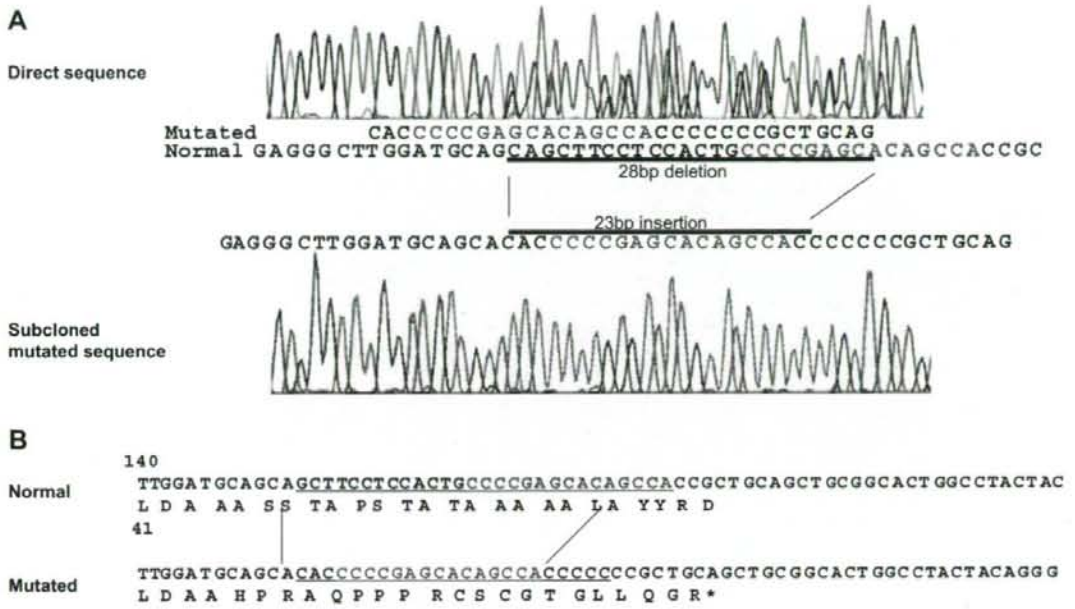

Fig. 3. Mutational analysis of the *GATA1* gene. (A) Sequence analysis was performed directly and using subcloned polymerase chain reaction product and showed a deletion–insertion mutation (28-bp deletion and 23-bp insertion) between 152 and 179 within exon 2. (B) This deletion–insertion mutation introduced a premature stop codon after Arg64. Numbers represent nucleotides from the 5′ end of exon 2.

has been reported by several authors and appears to represent a nonrandom chromosomal abnormality in patients with MDS/AML and Down syndrome [14,17]. Partial trisomy of 7q [8] or monosomy 1 [18,19] have also been reported. Unbalanced translocation t(1;7) in childhood myelodysplasia has been reported [20]. It is also possible that the t(1;7) played some role in the development of the MDS [21]. The mechanism of formation of the der(7)t(1;7) and its role in leukemogenesis are still unclear. Given that der(7)t(1;7) results in partial trisomy of 1q and partial monosomy of 7q, the increased dosage of the oncogenes located at 1q or the loss of the tumor suppressor genes located at 7q (or both factors) may be implicated in leukemogenesis of MDS and AML with der(7)t(1;7).

Cases of TAM usually have no karyotypic abnormality [1], but AMKL is associated with chromosomal abnormalities, including 8 trisomy and 19 trisomy [2]. Rare TAM cases have had chromosome abnormalities that were also observed in developing AMKL [22]. As for the *GATA1* gene, the deletion–insertion mutations within exon 2 in our patient have been reported previously in only two cases of TAM [5,7]. Reciprocal translocations are rare in TAM with Down syndrome. In the present case, a der(7)t(1;7) with partial trisomy of 1q, which is among the most frequently observed abnormalities in Down syndrome, might contribute to evolution to acute leukemia. The present report contributes insight into the mechanism of leukemic transformation from TAM in Down syndrome.

Acknowledgments

This work was supported by a grant-in-aid for cancer research from the Ministry of Health, Labor, and Welfare of Japan.

References

[1] Hayashi Y, Hanada R, Yamamoto K, Ohde S, Niitsu N, Eguchi M, Sugita K, Nakazawa S. Transient megakaryoblastic proliferation in a newborn infant with Down's syndrome. Cancer Genet Cytogenet 1987;28:373–4.

[2] Hayashi Y, Eguchi M, Sugita K, Nakazawa S, Sato T, Kojima S, Bessho F, Konishi S, Inaba T, Hanada R. Cytogenetic findings and clinical features in acute leukemia and transient myeloproliferative disorder in Down's syndrome. Blood 1988;72:15–23.

[3] Hitzler JK, Zipursky A. Origins of leukaemia in children with Down syndrome. Nat Rev Cancer 2005;5:11–20.

[4] Wechsler J, Greene M, McDevitt MA, Anastasi J, Karp JE, Le Beau MM, Crispino JD. Acquired mutations in *GATA1* in the megakaryoblastic leukemia of Down syndrome. Nat Genet 2002;32: 148–52.

[5] Rainis L, Bercovich D, Strehl S, Teigler-Schlegel A, Stark B, Trka J, Amariglio N, Biondi A, Muler I, Rechavi G, Kempski H, Haas OA, Izraeli S. Mutations in exon 2 of *GATA1* are early events in megakaryocytic malignancies associated with trisomy 21. Blood 2003;102: 981–6.

[6] Xu G, Nagano M, Kanezaki R, Toki T, Hayashi Y, Taketani T, Taki T, Mitui T, Koike K, Kato K, Imaizumi M, Sekine I, Ikeda Y, Hanada R, Sako M, Kudo K, Kojima S, Ohneda O, Yamamoto M, Ito E. Frequent mutations in the *GATA-1* gene in the transient myeloproliferative disorder of Down syndrome. Blood 2003;102:2960–8.

[7] Hitzler JK, Cheung J, Li Y, Scherer SW, Zipursky A. *GATA1* mutations in transient leukemia and acute megakaryoblastic leukemia of Down syndrome. Blood 2003;101:4301–4.

[8] Bunin N, Nowell PC, Belasco J, Shah N, Willoughby M, Farber PA, Lange B. Chromosome 7 abnormalities in children with Down syndrome and preleukemia. Cancer Genet Cytogenet 1991;54:119–26.

[9] Sawyer JR, Roloson GJ, Head DR, Becton D. Karyotype evolution in a patient with Down syndrome and acute leukemia following a congenital leukemoid reaction. Med Pediatr Oncol 1994;22:404–9.

[10] Zipursky A, Wang H, Brown EJ, Squire J. Interphase cytogenetic analysis of in vivo differentiation in the myelodysplasia of Down syndrome. Blood 1994;84:2278–82.

[11] Yamaguchi Y, Fujii H, Kazama H, Iinuma K, Shinomiya N, Aoki T. Acute myeloblastic leukemia associated with trisomy 8 and translocation 8;21 in a child with Down syndrome. Cancer Genet Cytogenet 1997;97:32–4.

[12] Duflos-Delaplace D, Lai JL, Nelken B, Genevieve F, Defachelles AS, Zandecki M. Transient leukemoid disorder in a newborn with Down syndrome followed 19 months later by an acute myeloid leukemia: demonstration of the same structural change in both instances with clonal evolution. Cancer Genet Cytogenet 1999;113:166–71.

[13] Kojima S, Sako M, Kato K, Hosoi G, Sato T, Ohara A, Koike K, Okimoto Y, Nishimura S, Akiyama Y, Yoshikawa T, Ishii E, Okamura J, Yazaki M, Hayashi Y, Eguchi M, Tsukimoto I, Ueda K. An effective chemotherapeutic regimen for acute myeloid leukemia and myelodysplastic syndrome in children with Down's syndrome. Leukemia 2000;14:786–91.

[14] Creutzig U, Ritter J, Vormoor J, Ludwig WD, Niemeyer C, Reinisch I, Stollmann-Gibbels B, Zimmermann M, Harbott J. Myelodysplasia and acute myelogenous leukemia in Down's syndrome: a report of 40 children of the AML-BFM Study Group. Leukemia 1996;10:1677–86.

[15] Kaneko Y, Rowley JD, Variakojis D, Chilcote RR, Moohr JW, Patel D. Chromosome abnormalities in Down's syndrome patients with acute leukemia. Blood 1981;58:459–66.

[16] de Alarcon PA, Patil S, Golberg J, Allen JB, Shaw S. Infants with Down's syndrome: use of cytogenetic studies and in vitro colony assay for granulocyte progenitor to distinguish acute nonlymphocytic leukemia from a transient myeloproliferative disorder. Cancer 1987;60:987–93.

[17] Litz CE, Davies S, Brunning RD, Kueck B, Parkin JL, Gajl Peczalska K, Arthur DC. Acute leukemia and the transient myeloproliferative disorder associated with Down syndrome: morphologic, immunophenotypic and cytogenetic manifestations. Leukemia 1995;9:1432–9.

[18] Blann MM, Morgan DL, Oblender M, Heinen B, Williams J, Tonk VS. Duplication of 1q in a child with Down syndrome and myelodysplastic syndrome. Cancer Genet Cytogenet 2000;119:74–6.

[19] Suarez CR, Le Beau MM, Silberman S, Fresco R, Rowley JD. Acute megakaryoblastic leukemia in Down's syndrome: report of a case and review of cytogenetic findings. Med Pediatr Oncol 1985;13:225–31.

[20] Horsman DE, Massing BG, Chan KW, Kalousek DK. Unbalanced translocation (1;7) in childhood myelodysplasia. Am J Hematol 1988;27:174–8.

[21] Hoo JJ, Szego K, Jones B. Confirmation of centromeric fusion in 7p/1q translocation associated with myelodysplastic syndrome. Cancer Genet Cytogenet 1992;64:186–8.

[22] Zipursky A. Transient leukaemia: a benign form of leukaemia in newborn infants with trisomy 21. Br J Haematol 2003;120:930–8.

bjh research paper

Prospective monitoring of *BCR-ABL1* transcript levels in patients with Philadelphia chromosome-positive acute lymphoblastic leukaemia undergoing imatinib-combined chemotherapy

Masamitsu Yanada,[1] Isamu Sugiura,[2] Jin Takeuchi,[3] Hideki Akiyama,[4] Atsuo Maruta,[5] Yasunori Ueda,[6] Noriko Usui,[7] Fumiharu Yagasaki,[8] Toshiaki Yujiri,[9] Makoto Takeuchi,[10] Kazuhiro Nishii,[11] Yukihiko Kimura,[12] Shuichi Miyawaki,[13] Hiroto Narimatsu,[1] Yasushi Miyazaki,[14] Shigeki Ohtake,[15] Itsuro Jinnai,[8] Keitaro Matsuo,[16] Tomoki Naoe[1] and Ryuzo Ohno[16] for the Japan Adult Leukemia Study Group

[1]Nagoya University Graduate School of Medicine, Nagoya, [2]Toyohashi Municipal Hospital, Toyohashi, [3]Nihon University School of Medicine, [4]Tokyo Metropolitan Komagome Hospital, Tokyo, [5]Kanagawa Cancer Centre, Yokohama, [6]Kurashiki Central Hospital, Kurashiki, [7]Jikei University School of Medicine, Tokyo, [8]Saitama Medical University International Medical Centre, Saitama, [9]Yamaguchi University School of Medicine, Yamaguchi, [10]National Hospital Organization Minami-Okayama Medical Centre, Okayama, [11]Mie University Graduate School of Medicine, Tsu, [12]Tokyo Medical University, Tokyo, [13]Saiseikai Maebashi Hospital, Maebashi, [14]Nagasaki University Graduate School of Biomedical Sciences, Nagasaki, [15]Kanazawa University Graduate School of Medical Science, Kanazawa, and [16]Aichi Cancer Centre, Nagoya, Japan

Received 2 June 2007; accepted for publication 11 July 2008

Correspondence: Masamitsu Yanada MD, Department of Hematology and Oncology, Nagoya University Graduate School of Medicine, 65 Tsurumai, Showa-ku, Nagoya 466-8550, Japan.
E-mail: myanada@mte.biglobe.ne.jp

Summary

The clinical significance of minimal residual disease (MRD) is uncertain in patients with Philadelphia chromosome-positive acute lymphoblastic leukaemia (Ph+ ALL) treated with imatinib-combined chemotherapy. Here we report the results of prospective MRD monitoring in 100 adult patients. Three hundred and sixty-seven follow-up bone marrow samples, collected at predefined time points during a uniform treatment protocol, were analysed for *BCR-ABL1* transcripts by quantitative reverse transcription polymerase chain reaction. Ninety-seven patients (97%) achieved complete remission (CR), and the relapse-free survival (RFS) rate was 46% at 3 years. Negative MRD at the end of induction therapy was not associated with longer RFS or a lower relapse rate ($P = 0{\cdot}800$ and $P = 0{\cdot}964$ respectively). Twenty-nine patients showed MRD elevation during haematological CR. Of these, 10 of the 16 who had undergone allogeneic haematopoietic stem cell transplantation (HSCT) in first CR were alive without relapse at a median of 2·9 years after transplantation, whereas 12 of the 13 who had not undergone allogeneic HSCT experienced a relapse. These results demonstrate that, in Ph+ ALL patients treated with imatinib-combined chemotherapy, rapid molecular response is not associated with a favourable prognosis, and that a single observation of elevated MRD is predictive of subsequent relapse, but allogeneic HSCT can override its adverse effect.

Keywords: acute lymphoblastic leukaemia, Philadelphia chromosome, *BCR-ABL1*, imatinib, minimal residual disease.

The recent development of imatinib-combined chemotherapy has drastically improved overall treatment results in Philadelphia chromosome-positive acute lymphoblastic leukaemia (Ph+ ALL) (Ottmann & Wassmann, 2005; Yanada & Naoe, 2006; Thomas, 2007). Nearly 95% of newly diagnosed patients now achieve complete remission (CR) (Thomas *et al*, 2004;

 First published online 2 October 2008
British Journal of Haematology, **143**, 503–510 doi:10.1111/j.1365-2141.2008.07377.x

Lee *et al*, 2005; Wassmann *et al*, 2006; Yanada *et al*, 2006). However, outcome after CR depends on the individual patient and is not predictable. Young patients generally undergo allogeneic haematopoietic stem cell transplantation (HSCT) after achieving CR if a suitable donor is available, based on the concept that it is the established treatment with curative potential for this disease (Cornelissen *et al*, 2001; Dombret *et al*, 2002; Stirewalt *et al*, 2003; Yanada *et al*, 2005). Nevertheless, a fraction of patients experience a relapse even prior to transplantation, whereas some remain alive in remission for years without undergoing HSCT.

Minimal residual disease (MRD), as measured by reverse transcription-polymerase chain reaction (RT-PCR) or flow cytometry, has been shown to be useful for predicting prognosis in paediatric (Brisco *et al*, 1994; Cave *et al*, 1998; Coustan-Smith *et al*, 1998; van Dongen *et al*, 1998; Dworzak *et al*, 2002; Nyvold *et al*, 2002; Zhou *et al*, 2007) and adult ALL patients (Brisco *et al*, 1996; Mortuza *et al*, 2002; Vidriales *et al*, 2003; Bruggemann *et al*, 2006; Raff *et al*, 2007). However, the utility of MRD as a prognostic indicator has been established on the basis of data from patients treated with chemotherapy alone, and it remains to be determined whether it is useful in patients treated with chemotherapy in combination with imatinib. The Japan Adult Leukemia Study Group (JALSG) recently conducted a phase II trial of imatinib-combined chemotherapy in newly diagnosed Ph+ ALL patients (Towatari *et al*, 2004; Yanada *et al*, 2006, 2008). In that trial, *BCR-ABL1* transcript levels in bone marrow were prospectively monitored at predetermined time points using quantitative real-time RT-PCR (RQ-PCR). The results are presented here, with particular emphasis on the prognostic significance of rapid MRD clearance and MRD kinetics.

Patients and methods

Patients

The patient eligibility requirements of the phase II trial were as follows: newly diagnosed with Ph+ ALL, aged 15–64 years, an Eastern Cooperative Oncology Group performance status of 0–3, and adequate liver, kidney and heart function. Written informed consent was obtained from all patients prior to registration. The protocol was reviewed and approved by the institutional review boards of all of participating centres and was conducted in accordance with the Declaration of Helsinki. This trial was registered at http://www.clinicaltrials.gov as #NCT00130195.

The treatment schedule is summarized in Table I. Allogenic HSCT was allowed after achieving CR if the patient had a suitable donor. The original target sample size was 77 patients (Yanada *et al*, 2006), with the CR rate defined as the primary endpoint. Eighty patients had been enrolled by January 2005, when enrolment was extended to 100 patients to attain a more precise point estimate of the overall survival (OS) rate. This sample size enabled the lower limit of the 95% confidence interval (CI) of OS rate (expected to be 70% at 1 year) to be higher than 60%.

MRD evaluation

Molecular monitoring was performed with use of the RQ-PCR assay in a single independent laboratory. Bone marrow samples were collected at diagnosis; at days 28 and 63 of the induction course; after the first, second, fifth and sixth consolidation courses; after 1 year of treatment; and at the end of therapy (2 years from the date of CR).

Total RNA was extracted from mononuclear cells using the QIAamp RNA blood mini kit (Qiagen GmbH, Hilden, Germany) according to the manufacturer's instructions. The concentration and purity of RNA were measured by spectrophotometric determination of the A260/A280 ratio. Total RNA (1·5 μg) was transcribed to cDNA in a 22·5-μl reaction mixture containing 500 ng of random hexamer (Invitrogen, Carlsbad, CA, USA), 50 units of reverse transcriptase (Invitrogen), 40 units of RNase inhibitor (Invitrogen) and 500 μmol/l dNTP. The reaction mixture (total volume: 50 μl) contained 7·5 μl of a 22·5-μl RNA mixture (corresponding to 500 ng of RNA), 15 pmol of forward and reverse primers, 10 pmol of TaqMan probe, and 25 μl of 2× TaqMan universal PCR master mix (Applied Biosystems, Foster City, CA, USA). The primer and probe sequences have been described elsewhere (Towatari *et al*, 2004). Amplification was carried out with an initial activation of the polymerase at 50°C for 2 min and 95°C for 10 min, followed by 50 cycles consisting of two steps: 95°C for 15 s and 60°C for 1 min. Fluorescent emission spectra were monitored every 7 s and analysed using the PRISM 7700 system with SEQUENCE DETECTION SYSTEM software (version 1.7; Applied Biosystems). Amplified cDNA fragments were cloned into the pCRII vector (Invitrogen) and used as the reference standard. The copy number of each plasmid was calculated from the DNA concentration (determined by measuring A260) and the molecular weight of the plasmid. The copy number of the *BCR-ABL1* transcripts was calculated by comparing the C_t values of samples with those of the standard and converted to molecules per microgram RNA after being normalized by means of *GAPDH*. The threshold for quantification was 50 copies/μg RNA, which corresponded to a minimal sensitivity of 10^{-5}. Detectable MRD levels below this threshold were referred to as '<50 copies/μg' to distinguish from undetectable MRD. Nested PCR was not performed in this study. Samples with *GAPDH* levels below $5{\cdot}7 \times 10^5$ copies/μg RNA were not eligible for MRD evaluation.

Statistical analysis

Relapse-free survival (RFS) was defined as the time from CR to relapse, death, or last follow-up, and OS was defined as the time from registration to death or last follow-up. A Kaplan–Meier survival analysis was performed to estimate the probabilities of RFS and OS, with differences between the curves